TTP09-07 March 2009

Three Lectures on Meson Mixing and CKM phenomenology[1]

Ulrich Nierste

Institut für Theoretische Teilchenphysik
Universität Karlsruhe
Karlsruhe Institute of Technology,
D-76128 Karlsruhe, Germany

Abstract

I give an introduction to the theory of meson-antimeson mixing, aiming at students who plan to work at a flavour physics experiment or intend to do associated theoretical studies. I derive the formulae for the time evolution of a neutral meson system and show how the mass and width differences among the neutral meson eigenstates and the CP phase in mixing are calculated in the Standard Model. Special emphasis is laid on CP violation, which is covered in detail for $K-\overline{K}$ mixing, $B_d-\overline{B}_d$ mixing and $B_s-\overline{B}_s$ mixing. I explain the constraints on the apex $(\overline{\rho},\overline{\eta})$ of the unitarity triangle implied by ϵ_K, ΔM_{B_d}, $\Delta M_{B_d}/\Delta M_{B_s}$ and various mixing-induced CP asymmetries such as $a_{\rm CP}(\overline{B}_d \to J/\psi K_{\rm short})(t)$. The impact of a future measurement of CP violation in flavour-specific B_d decays is also shown.

Contents

[1]Contribution to the *Helmholtz International Summer School "Heavy quark physics"*, Bogoliubov Laboratory of Theoretical Physics, Dubna, Russia, August 11-21, 2008.

1 First lecture: A big-brush picture

1.1 Mesons, quarks and box diagrams

The neutral K, D, B_d and B_s mesons are the only hadrons which mix with their antiparticles. These meson states are flavour eigenstates and the corresponding antimesons $\overline{K}$, $\overline{D}$, $\overline{B}_d$ and $\overline{B}_s$ have opposite flavour quantum numbers:

$$\begin{array}{llll} K \sim \overline{s}d, & D \sim c\overline{u}, & B_d \sim \overline{b}d, & B_s \sim \overline{b}s, \\ \overline{K} \sim s\overline{d}, & \overline{D} \sim \overline{c}u, & \overline{B}_d \sim b\overline{d}, & \overline{B}_s \sim b\overline{s}, \end{array} \qquad (1)$$

Here for example "$B_s \sim \overline{b}s$" means that the B_s meson has the same flavour quantum numbers as the quark pair $(\overline{b}, s)$, i.e. the beauty and strangeness quantum numbers are $B = 1$ and $S = -1$, respectively. The meson states in Eq. (1) are also eigenstates of the strong and electromagnetic interactions. As long as we neglect the weak interaction, they are also mass eigenstates, with the same mass for meson and antimeson. In the Standard Model (SM) all interaction vertices conserve flavour, except for the couplings of W bosons to fermions.[2] The piece of the SM Lagrangian which describes the W couplings to quarks reads

$$\mathcal{L}_W = \frac{g_w}{\sqrt{2}} \sum_{j,k=1,2,3} \left[V_{jk}\, \overline{u}_{jL}\, \gamma^\mu d_{kL}\, W_\mu^+ + V_{jk}^*\, \overline{d}_{kL}\, \gamma^\mu u_{jL}\, W_\mu^- \right]. \qquad (2)$$

Here g_w is the weak coupling constant and V is the 3×3 unitary *Cabibbo-Kobayashi-Maskawa (CKM) matrix*:

$$V \;=\; \left(\begin{array}{ccc} V_{ud} & V_{us} & V_{ub} \\ V_{cd} & V_{cs} & V_{cb} \\ V_{td} & V_{ts} & V_{tb} \end{array} \right). \qquad (3)$$

In Eq. (2) I have further used the notations $(d_1, d_2, d_3) = (d, s, b)$ and $(u_1, u_2, u_3) = (u, c, t)$. The W boson only couples to the left-handed components of the quark fields as indicated by the subscript "L" in Eq. (2). At fourth order in the weak coupling we can change the flavour quantum numbers by two units and obtain transitions between mesons and antimesons. The corresponding Feynman diagrams are shown in Fig. 1. These $|\Delta F| = 2$ diagrams, where F denotes the appropriate flavour

[2] Strictly speaking, this statement assumes that the so-called unitary gauge for the weak gauge bosons is adopted. The unphysical charged pseudo-Goldstone bosons, which appear in other gauges, also have flavour-changing vertices. Changing the gauge shuffles terms between the pseudo-Goldstone bosons and the longitudinal components of the gauge bosons.

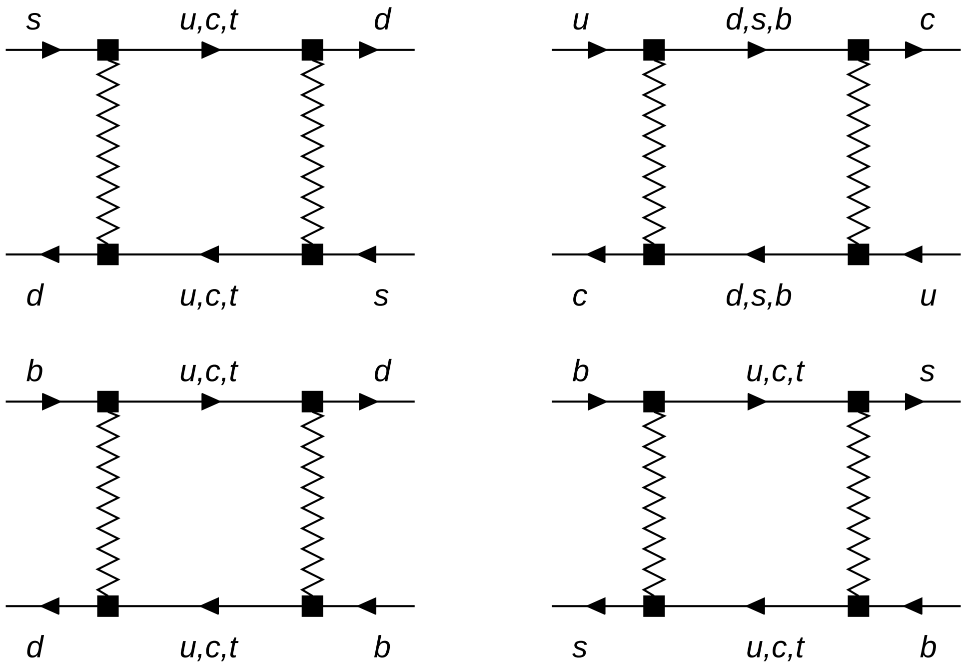

Figure 1: Box diagrams for $K-\overline{K}$, $D-\overline{D}$, $B_d-\overline{B}_d$ and $B_s-\overline{B}_s$ mixing. The zigzag lines represent W bosons. For each process there is also a second box diagram, obtained by a 90° rotation.

quantum number $F = S$, C or B, represent the lowest non-vanishing contribution to the transition matrix element Σ_{12} defined by

$$-i(2\pi)^4\delta^{(4)}(p_M - p_{\overline{M}})\Sigma_{12} \;=\; \frac{\langle M(\vec{p}_M)|S|\overline{M}(\vec{p}_{\overline{M}})\rangle}{2M_M} \tag{4}$$

with the S-matrix S and the generic notation $M = K,D,B_d$ or B_s. (The notation Σ_{12} refers to the quantum-mechanical two-state system with $|1\rangle = |M\rangle$ and $|2\rangle = |\overline{M}\rangle$.) I comply with the standard relativistic normalisation of the meson states, $\langle M(\vec{p}\,')|M(\vec{p})\rangle = 2E\,(2\pi)^3\delta^{(3)}(\vec{p}\,' - \vec{p})$. The meson mass $M_M = \sqrt{E^2 - \vec{p}^{\,2}}$ in the denominator in Eq. (4) is introduced for later convenience. In terms of the Hamiltonian (density) $H_{\rm int}^{SM}(x) = -\mathcal{L}_{\rm int}^{SM}(x)$, which encodes all interactions of the SM, the S-matrix is given by the usual time-ordered exponential

$$S \;=\; \mathbf{T}e^{-i\int d^4x H_{\rm int}^{\rm SM}(x)}. \tag{5}$$

In order to link Eqs. (4) and (5) to the diagrams of Fig. 1 we must consider the contribution from $\mathcal{L}_W$ in Eq. (2) to $-H_{\rm int}^{SM}$ and expand the time-ordered exponential in Eq. (5) to order g_w^4. The determination of this term amounts to the calculation of the two contributing box diagrams with the usual Feynman rules of the weak interaction. To this point we have only used standard text-book quantum field theory, noting an important omission: No effect of the strong interaction has been taken into account by now. Most importantly, we do not know yet how to take care of quark confinement, which forces the external quarks in the diagrams of Fig. 1 to form mesons. As an important feature, Quantum Chromodynamics (QCD) behaves very differently at short and long distances: At short distances (probed by large energies) the QCD coupling constant g_s is small and we can apply perturbation theory [1], just as we did with the weak interaction. That is, effects of short-distance QCD can be included by adding gluons to the diagrams in Fig. 1. At large distances, corresponding to low energies, QCD is non-perturbative and one must resort to different methods, such as lattice gauge theory or QCD sum rules. Long-distance QCD is also referred to as *hadronic physics*, because its degrees of freedom are hadrons rather than quarks and gluons. In many cases the associated theoretical uncertainties are the main obstacle in the relation between measured quantities and the fundamental parameters of nature encoded in the Lagrangian $\mathcal{L}$. Theorists pursue a two-fold strategy to deal with hadronic uncertainties: On one hand they try to refine non-perturbative methods such as lattice gauge theory. On the other hand they try to identify quantities in which hadronic uncertainties are small or even absent or look for ways to eliminate hadronic uncertainties through clever combinations of different observables. We will encounter both strategies in our discussion of meson-antimeson mixing. Weak processes of hadrons involve several largely-separated energy scales.[3] For example, in $B-\overline{B}$ mixing we encounter $m_t > M_W \gg m_b \gg \Lambda_{\rm QCD}$, where $\Lambda_{\rm QCD} \sim 0.4\,$GeV is the fundamental scale of the strong interaction governing e.g. the size of binding energies. In order to correctly calculate Σ_{12} we must separate the different scales from each other and apply different computational methods to large and small energy scales. However, without detailed understanding of the strong interaction we can roughly assess the relative importance of the contributions from the different internal quark flavours in Fig. 1: In the case of $B_d-\overline{B}_d$ mixing and $B_s-\overline{B}_s$ mixing one finds that the box diagram with internal top quarks vastly dominates over the diagrams with light quarks, because the result of the diagram grows with the internal quark mass. For $K-\overline{K}$ mixing and $D-\overline{D}$ mixing no such estimate is possible, because the contribution with the heaviest quark is suppressed by small CKM elements.

Owing to $\Sigma_{12} \neq 0$, M and $\overline{M}$ mix and are no more mass eigenstates. The latter are obtained by diagonalising the 2×2 matrix Σ_{ij}, where

$$-i(2\pi)^4 \delta^{(4)}(p_i' - p_j)\Sigma_{ij} \;\;=\;\; \frac{\langle i, \vec{p}_i{}' | S^{\rm SM} | j, \vec{p}_j \rangle}{2 M_M} \tag{6}$$

with $|1, \vec{p}_1\rangle = |M(\vec{p}_1)\rangle$ and $|2, \vec{p}_2\rangle = |\overline{M}(\vec{p}_2)\rangle$ generalises Eq. (4). We list two important aspects of meson-antimeson mixing:

i) The two mass eigenstates are linear combinations of M and $\overline{M}$. The degeneracy is lifted and we can denote the two mass eigenstates by M_H and M_L, where "H" and "L" stand for "heavy" and "light", respectively. M_H and M_L not only differ in their masses, but also in their lifetimes.

ii) If we produce a meson M at some time $t = 0$, the corresponding state will evolve into a superposition of M and $\overline{M}$ at later times $t > 0$. One observes meson-antimeson oscillations.

We will calculate the differences among the masses and decay widths in the second and third lectures. Studies of neutral Kaons mainly exploit property i), while the mixings of the other three neutral meson systems are investigated through property ii). The reason for the Kaon's special role here is the vast lifetime difference between K_H and K_L. The former state, usually denoted as $K_{\rm long}$, lives roughly 500 times longer than $K_L = K_{\rm short}$, so that one can easily produce a $K_{\rm long}$ beam. For D, B_d and B_s mesons the width differences are much smaller than the average decay width of the two eigenstates and this method is not feasible. The identification of the meson (discriminating between M and $\overline{M}$)

[3] I use natural (or Planck) units with $\hbar = c = 1$, so that masses and momenta have units of GeV.

needed to track the meson-antimeson oscillations is called *flavour tagging*. To observe the oscillations the mesons must move sufficiently fast in the detector. Modern B factories, which produce $(B_d, \overline{B}_d)$ pairs via the $\Upsilon(4S)$ resonance, have therefore asymmetric beam energies, so that the centre-of-mass frame (coinciding with the rest frame of the $\Upsilon(4S)$) moves with respect to the laboratory frame. At hadron colliders studies of meson-antimeson oscillations profit from the large boost of the produced mesons. Tevatron and LHC are especially powerful for B_s physics, because the $B_s - \overline{B}_s$ oscillations are very rapid.

1.2 A bit of history

Meson-antimeson mixings belong to the class of *flavour-changing neutral current (FCNC)* processes, which involve different flavours with the same electric charge. Since in the SM such processes are forbidden at tree-level, they are sensitive to new heavy particles appearing as virtual particles in loop diagrams. Historically, the first new particle predicted from the consideration of FCNCs was the charm quark, which was needed to eliminate large tree-level FCNC couplings in conflict with experiment [2]. Subsequently, the rough size of the charm quark mass m_c was predicted from the size of the mass difference $\Delta M_K = M_H - M_L$ in the neutral Kaon system [3]. A great success story of flavour physics has been the exploration of the discrete symmetries charge conjugation (C), parity (P) and time reversal (T). Charged Kaon decays had revealed in 1956 that P and C are not conserved by the weak interaction, while physicists kept their faith in a good *CP* symmetry. If *CP* were conserved, we could assign *CP* quantum numbers to $K_{\rm long}$ and $K_{\rm short}$. The latter meson was observed to decay into a two-pion state, and each pion is *CP*-odd and contributes a factor of -1 to the total *CP* quantum number (which is multiplicative). A further contribution to the *CP* quantum number of a two-particle state stems from the angular momentum: States with orbital angular momentum quantum number l involve the spherical harmonic $Y^l_m(\vec{n})$, where $\vec{n} = \vec{p}/|\vec{p}|$ and $\vec{p}$ is the relative momentum of the two particles considered. Since $Y^l_m(\vec{n}) = (-1)^l Y^l_m(-\vec{n})$, states with odd l have P and *CP* quantum numbers -1, while those with even l are even under P and *CP*. Since the decaying Kaon has no spin and the total angular momentum is conserved in any decay process, the two pions in the final state have have $l = 0$ in the Kaon rest frame. (In general the spin wave function also matters, but pions have spin zero.) In total we find that the two-pion state is *CP*-even. Now $K_{\rm long}$ was only seen to decay into three pions, so that this meson was believed to be *CP*-odd. In fact, its long lifetime stems from the kinematical suppression of the decay into the *CP*-odd three–pion state. To understand that a three-pion state is always *CP*-odd, first note that we get a contribution of $(-1)^3 = -1$ from the intrinsic *CP* quantum numbers of the three pions. Next pick any two of the pions and call there relative orbital angular momentum quantum number l_1. Likewise we denote the quantum number for the relative orbital angular momentum between this pair and the third pion by l_2. One of the selection rules for the addition of angular momenta implies that the total quantum number l satisfies $l \geq |l_1 - l_2|$. Since $l = 0$, this means that $l_1 = l_2$ and the "orbital" contribution to the *CP* quantum number is $(-1)^{l_1+l_2} = (-1)^{2l_1} = 1$. Thus the three-pion state is *CP*-odd, irrespective of the value of l_1.

In 1964 the decay $K_{\rm long} \to \pi\pi$ was observed, establishing *CP* violation [4]. The two-generation Standard Model, whose construction was completed later in that decade [5], could not accommodate this phenomenon: We will see below that *CP*-violating interactions of quarks necessarily involve complex couplings. While the V_{jk}'s in Eq. (2) are a priori complex, one can render them real in the two-generation SM by transforming the quark fields as

$$d_j \to e^{i\phi_j^d} d_j, \qquad\qquad u_k \to e^{i\phi_k^u} u_k. \tag{7}$$

with appropriate phases ϕ_j^d and ϕ_k^u. The net effects of these rephasings are the replacements of the V_{jk}'s by

$$V_{jk} e^{i(\phi_j^d - \phi_k^u)}. \tag{8}$$

These expressions involves three independent phases and we may choose e.g. $\phi_1^d - \phi_1^u$, $\phi_1^d - \phi_2^u$ and $\phi_2^d - \phi_1^u$ in such a way that the three complex phases of a unitarity 2×2 matrix are eliminated, arriving at the real Cabibbo matrix. In 1973 Kobayashi and Maskawa have pointed out that a physical *CP*-violating phase persists in the quark mixing matrix, if there are at least three generations [6]: A unitary 3×3 matrix has 6 complex phases while we have only 5 phase differences $\phi_j^d - \phi_k^u$ at our disposal. The finding of Kobayashi and Maskawa was largely ignored at that time and only appreciated after the third fermion generation was experimentally established. In 1987 the ARGUS experiment at DESY observed $B_d - \overline{B}_d$ mixing, at an unexpectedly large rate [7]. This finding was the first hint at a truly heavy top quark, which enters the lower left box diagram of Fig. 1.

1.3 *CP* violation

The last stroke of the brush is devoted to *CP* violation. Defining

$$CP|\, M(\vec{p}_{\overline{M}})\rangle \;=\; -|\,\overline{M}(-\vec{p}_{\overline{M}})\rangle, \qquad\qquad CP|\,\overline{M}(\vec{p}_{\overline{M}})\rangle \;=\; -|\, M(-\vec{p}_{\overline{M}})\rangle \tag{9}$$

we first look at decays $M \to f_{\rm CP}$ and $\overline{M} \to f_{\rm CP}$, where $f_{\rm CP}$ is a *CP* eigenstate:

$$CP|f_{\rm CP}\rangle \;=\; \eta_{\rm CP}|f_{\rm CP}\rangle \tag{10}$$

with $\eta_{\rm CP} = \pm 1$. The *CP* operator appearing in Eqs. (9) and (10) is unitary, i.e. $(CP)^{-1} = (CP)^{\dagger}$. To get an idea of the importance of meson-antimeson mixing for the study of *CP* violation we first assume that M and $\overline{M}$ do not mix. We could still measure the decay rates of the *CP*-conjugate processes $M \to f_{\rm CP}$ and $\overline{M} \to f_{\rm CP}$. If we find them different we establish *direct CP violation* (often called *CP violation in decay*). However, it is very difficult to relate a direct *CP* asymmetry to a fundamental *CP* phase in $\mathcal{L}$: A non-zero direct *CP* asymmetry also requires final state interaction related to the rescattering process $M \to f'_{\rm CP} \to f_{\rm CP}$. Rescattering leads to *CP*-conserving complex phases in the decay amplitude. In the absence of such phases the amplitudes of $M \to f_{\rm CP}$ and $\overline{M} \to f_{\rm CP}$ would simply be related by complex conjugation since all phases would switch sign under CP. But then the two decay amplitudes would have the same magnitude leading to identical decay rates. For $M = D, B_d, B_s$ this hadronic rescattering process is mainly inelastic and intractable with present theoretical methods.

But thanks to meson-antimeson mixing we can study meson states which are superpositions of $|M\rangle$ and $|\overline{M}\rangle$. The mass eigenstates $|M_H\rangle$ and $|M_L\rangle$ are linear combinations of $|M\rangle$ and $|\overline{M}\rangle$:

$$\begin{aligned} |M_L\rangle &= p|M\rangle + q|\overline{M}\rangle\,, \\ |M_H\rangle &= p|M\rangle - q|\overline{M}\rangle\,, \end{aligned} \tag{11}$$

with $|p|^2 + |q|^2 = 1$. We can calculate p and q from the box diagrams in Fig. 1 and will do so in the following sections. A commonly used shorthand notation for decay amplitudes is

$$A_f = A(M \to f) = \langle f|S|M\rangle, \qquad \overline{A}_f = A(\overline{M} \to f) = \langle f|S|\overline{M}\rangle. \tag{12}$$

A key quantity to study CP violation is the combination

$$\lambda_f = \frac{q}{p}\frac{\overline{A}_f}{A_f}. \tag{13}$$

λ_f encodes the essential feature of the interference of the $M \to f$ and $\overline{M} \to f$ decays, the relative phase between q/p (from meson-antimeson mixing) and $\overline{A}_f/A_f$ (stemming from the studied decay). In a first application, I discuss the decays of neutral Kaons into two charged or neutral pions. A neutral K or $\overline{K}$ meson state is a superposition of $K_H = K_{\rm long}$ and $K_L = K_{\rm short}$. At short times the decays of the $K_{\rm short}$ component of our Kaon beam will vastly dominate over the $K_{\rm long}$ decays and one can access the decay rates $\Gamma(K_{\rm short} \to \pi\pi)$ for $\pi\pi = \pi^+\pi^-, \pi^0\pi^0$. At large times, say, after 10 times the $K_{\rm short}$ lifetime, our beam is practically a pure $K_{\rm long}$ beam and we can study the CP-violating $\Gamma(K_{\rm long} \to \pi\pi)$ decays. It is advantageous to switch to the eigenbasis of strong isospin I:

$$\begin{aligned} |\pi^0\pi^0\rangle &= \sqrt{\frac{1}{3}}\,|\,(\pi\pi)_{I=0}\rangle - \sqrt{\frac{2}{3}}\,|\,(\pi\pi)_{I=2}\rangle\,, \\ |\pi^+\pi^-\rangle &= \sqrt{\frac{2}{3}}\,|\,(\pi\pi)_{I=0}\rangle + \sqrt{\frac{1}{3}}\,|\,(\pi\pi)_{I=2}\rangle\,, \end{aligned}$$

The strong interaction respects strong-isospin symmetry to an accuracy of typically 2%, so that we can neglect any rescattering between the $I = 0$ and $I = 2$ states. Consequently, no *direct CP* violation contributes to the famous CP-violating quantity

$$\epsilon_K \equiv \frac{\langle(\pi\pi)_{I=0}|K_{\rm long}\rangle}{\langle(\pi\pi)_{I=0}|K_{\rm short}\rangle}. \tag{14}$$

Abbreviating $A_0 \equiv A_{(\pi\pi)_{I=0}}$, $\overline{A}_0 \equiv \overline{A}_{(\pi\pi)_{I=0}}$ and (see Eq. (13)) $\lambda_0 \equiv \lambda_{(\pi\pi)_{I=0}}$ we insert Eq. (11) into Eq. (14) and readily find

$$\epsilon_K = \frac{1-\lambda_0}{1+\lambda_0}\,. \tag{15}$$

The experimental value [8]

$$\epsilon_K^{\rm exp} = e^{i\,\phi_\epsilon}\,(2.23 \pm 0.01) \times 10^{-3} \qquad \text{with} \quad \phi_\epsilon = (0.967 \pm 0.001)\,\frac{\pi}{4}\,. \tag{16}$$

therefore allows us to determine λ_0, which in our example is apparently close to 1. In our case with $|A_0| = |\overline{A}_0|$ (absence of direct CP violation) we have $|\lambda_0| = |q/p|$. With Eq. (15) we find

$$\epsilon_K \simeq \frac{1}{2}\,[1-\lambda_0] \;\simeq\; \frac{1}{2}\left(1 - \left|\frac{q}{p}\right| - i\,{\rm Im}\,\lambda_0\right) \tag{17}$$

up to corrections of order ϵ_K^2. Remarkably, from the real and imaginary part of ϵ_K we infer two CP-violating quantities:

i) the deviation of $|q/p|$ from 1 and

ii) the deviation of $\mathrm{Im}\,\lambda_0$ from 0.

The first quantity is independent of the studied final state f and codifies *CP violation in mixing*. The second quantity, $\mathrm{Im}\,\lambda_f$, measures *CP* violation in the interference of mixing and decay or, in short, *mixing-induced CP violation* in the decay $M \to f$.

In the case of D, B_d or B_s mixing studies one tags the flavour at some time $t = 0$. The corresponding meson states are called $|M(t)\rangle$ and $|\overline{M}(t)\rangle$ and satisfy $|M(t = 0)\rangle = |M\rangle$ and $|\overline{M}(t = 0)\rangle = |\overline{M}\rangle$. For $t > 0$ these time-dependent states are calculable superpositions of $|M\rangle$ and $|\overline{M}\rangle$ and by observing the time-dependence of $M(t) \to f$ we can infer λ_f. The presently most prominent application of this method is the precise determination of $\mathrm{Im}\,\lambda_f$ in the decay $B_d \to J/\psi K_{\mathrm{short}}$ by the B factories BaBar and BELLE. Needless to say that we will discuss this important topic in detail below.

While C, P, and T are violated in nature, the combination *CPT* is a good symmetry. This *CPT theorem* holds in any local Poincaré-invariant quantum field theory [9]. It implies that particles and antiparticles have the same masses and total decay widths. When applied to our mixing problem characterised by Σ in Eq. (6) the *CPT* theorem enforces $\Sigma_{11} = \Sigma_{22}$. However, while the *CPT* theorem implies $\Gamma_{\mathrm{tot}}(M) = \Gamma_{\mathrm{tot}}(\overline{M})$, one still has different time-integrated total decay rates for tagged mesons, $\int_0^\infty dt \Gamma_{\mathrm{tot}}(M(t)) \neq \int_0^\infty dt \Gamma_{\mathrm{tot}}(\overline{M}(t))$. This quantity is sensitive to the "arrow of time" and the difference $\Gamma_{\mathrm{tot}}(M(t)) - \Gamma_{\mathrm{tot}}(\overline{M}(t))$ measures *CP* violation rather than *CPT* violation. Throughout my lectures I assume *CPT* invariance and therefore identify *CP* symmetry with T symmetry. Still, experiments have tested the *CPT* theorem by probing $\Sigma_{11} = \Sigma_{22}$ in $K - \overline{K}$ mixing. We may speculate that Poincaré invariance and *CPT* symmetry are violated by the unknown dynamics of quantum gravity. If we are lucky the size of *CPT* violation scales linearly in the inverse Planck Mass M_{Planck}. Interestingly, today's accuracy of the *CPT* test $\Sigma_{11} = \Sigma_{22}$ is roughly M_K/M_{Planck}.

2 Second lecture: Time evolution

2.1 Time-dependent meson states

In the Schrödinger picture, the time evolution of a quantum-mechanical state $|\psi\rangle = |\psi, t = 0\rangle$ is given by $|\psi, t\rangle = \mathcal{U}(t, 0)|\psi\rangle$, with the unitary time-evolution operator $\mathcal{U}(t, 0)$. Consider first the case of a weakly-decaying charged meson (i.e. K^+, D^+ or B^+), which cannot mix with other states. The corresponding state at $t = 0$, $|M^+\rangle$, will evolve into a superposition of all states allowed by energy-momentum conservation. This class of states consists of the original meson state $|M^+\rangle$ and all final states $|f\rangle$ into which M^+ can decay. Defining

$$|M^+(t)\rangle = |M^+\rangle\langle M^+|\mathcal{U}(t, 0)|M^+\rangle \tag{18}$$

we can write

$$\mathcal{U}(t, 0)|M^+\rangle = |M^+(t)\rangle + \sum_f |f\rangle\langle f|\mathcal{U}(t, 0)|M^+\rangle.$$

In order to find $|M^+(t)\rangle$ we take a shortcut, by employing the exponential decay law to deduce

$$|M^+(t)\rangle = e^{-iM_M t} e^{-\Gamma t/2}|M^+\rangle \tag{19}$$

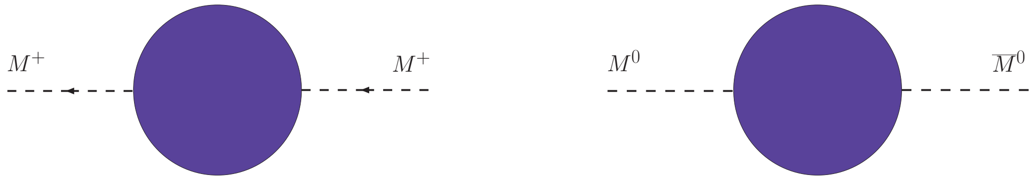

Figure 2: Left: generic self energy Σ of a charged meson. Right: $M^0-\overline{M}^0$ mixing amplitude Σ_{12}.

in the meson rest frame. The first term is the familiar time evolution factor of a stable state with energy $E = M_M$. The second factor involving the total width Γ is understood by considering the probability to find an undecayed meson at time t:

$$\left|\langle M^+|M^+(t)\rangle\right|^2 \;=\; e^{-\Gamma t}$$

Whenever I work in the Schrödinger picture I normalise the states as $\langle M^+|M^+\rangle = 1$. Since $M_M - i\Gamma/2$ is independent of t, we can compute it using the familiar covariant formulation of quantum field theory. The optical theorem tells us that M_M and $-\Gamma/2$ are given by the real and imaginary parts of the self-energy Σ (depicted in the left diagram of Fig. 2), where

$$-i(2\pi)^4\delta^{(4)}(\vec{p}\,' - \vec{p})\Sigma \;=\; \frac{\langle M^+(\vec{p}\,')|S|M^+(\vec{p})\rangle}{2M_M} \tag{20}$$

(To be precise, the diagram in Fig. 2 corresponds to $2M_M\Sigma$, so that $\Sigma = M_M - i\Gamma/2$ has mass dimension 1.) From Eq. (19) we find

$$i\frac{d}{dt}|M^+(t)\rangle \;=\; \left(M_M - i\frac{\Gamma}{2}\right)|M^+(t)\rangle. \tag{21}$$

This equation can be generalised to a two-state system describing neutral meson mixing:

$$i\frac{d}{dt}\begin{pmatrix} |M(t)\rangle \\ |\overline{M}(t)\rangle \end{pmatrix} \;=\; \Sigma\begin{pmatrix} |M(t)\rangle \\ |\overline{M}(t)\rangle \end{pmatrix} \tag{22}$$

where now Σ is the 2×2 matrix defined in Eq. (6). Recall that any matrix can be written as the sum of a hermitian and an antihermitian matrix. We write

$$\Sigma \;=\; M - i\,\frac{\Gamma}{2} \tag{23}$$

with the *mass matrix* $M = M^\dagger$ and the *decay matrix* $\Gamma = \Gamma^\dagger$. Then

$$M_{12} \;=\; \frac{\Sigma_{12} + \Sigma_{21}^*}{2}, \qquad\qquad \frac{\Gamma_{12}}{2} \;=\; i\,\frac{\Sigma_{12} - \Sigma_{21}^*}{2}. \tag{24}$$

The expressions on the RHS of Eq. (24) are called *dispersive* and *absorptive* parts of Σ_{12}, respectively. The right diagram in Fig. 2 generically represents all contributions to Σ_{12}. To compute Σ_{12} we can certainly use perturbation theory for the weak interaction (which to lowest order amounts to the calculation of the box diagram in Fig. 1), but we must take into account the non-perturbative nature of the strong binding forces. The diagonal elements M_{11} and M_{22} are the masses of M and $\overline{M}$ and are generated from the quark mass terms in $\mathcal{L}$ and from the binding energy of the strong interaction.

However, the off-diagonal elements $M_{12} = M_{21}^*$ and all elements of Γ stem from the weak interaction and are therefore tiny in comparison with M_{11} and M_{22}. The only reason why we can experimentally access M_{12} roots in the *CPT* theorem: *CPT* symmetry enforces

$$M_{11} \;=\; M_{22}, \qquad\qquad \Gamma_{11} \;=\; \Gamma_{22}, \tag{25}$$

so that the eigenvalues of Σ are exactly degenerate for $\Sigma_{12} = \Sigma_{21} = 0$. Even the smallest Σ_{12} can lift the degeneracy and can lead to large meson-antimeson mixing.

With our shortcut we have avoided to prove that Eq. (21) holds with time-independent M and Γ. In fact, Eq. (21) and the inferred exponential decay law in Eq. (19) are not valid exactly, but receive tiny (and phenomenologically irrelevant) corrections [10]. The same statement is true for Eqs. (22) and (23), a proper derivation of Eq. (22) using time-dependent perturbation theory for the weak interaction employs the so-called *Wigner-Weisskopf approximation* [11]. Corrections to this approximation have been addressed in Ref. [13] and are below the 10^{-10} level.

We now proceed with the solution of our Schrödinger equation in Eq. (22). Eq. (11) means that the eigenvectors of Σ in Eq. (6) are $(p,q)^T$ and $(p,-q)^T$. That is, Σ is diagonalised as

$$Q^{-1}\Sigma\, Q \;=\; \begin{pmatrix} M_L - i\Gamma_L/2 & 0 \\ 0 & M_H - i\Gamma_H/2 \end{pmatrix} \tag{26}$$

with

$$Q \;=\; \begin{pmatrix} p & p \\ q & -q \end{pmatrix} \qquad \text{and} \qquad Q^{-1} \;=\; \frac{1}{2pq}\begin{pmatrix} q & p \\ q & -p \end{pmatrix}. \tag{27}$$

The ansatz in Eq. (27) works because $\Sigma_{11} = \Sigma_{22}$. The mass eigenstates $|M_{L,H}(t)\rangle$ obey an exponential decay law as $|M^+(t)\rangle$ in Eq. (19) with (M_M, Γ) replaced by $(M_{L,H}, \Gamma_{L,H})$. Transforming back to the flavour basis gives

$$\begin{pmatrix} |M(t)\rangle \\ |\overline{M}(t)\rangle \end{pmatrix} \;=\; Q \begin{pmatrix} e^{-iM_L t - \Gamma_L t/2} & 0 \\ 0 & e^{-iM_H t - \Gamma_H t/2} \end{pmatrix} Q^{-1} \begin{pmatrix} |M\rangle \\ |\overline{M}\rangle \end{pmatrix} \tag{28}$$

I adopt the following definitions for the average mass and width and the mass and width differences of the mass eigenstates:

$$\begin{aligned} m &= \frac{M_H + M_L}{2} = M_{11} = M_{22}\,, & \Gamma &= \frac{\Gamma_L + \Gamma_H}{2} = \Gamma_{11} = \Gamma_{22}\,, \\ \Delta M &= M_H - M_L\,, & \Delta\Gamma &= \Gamma_L - \Gamma_H\,. \end{aligned} \tag{29}$$

Note that ΔM is positive by definition while $\Delta\Gamma$ can have either sign. Experimentally the sign of $\Delta\Gamma$ is only known for Kaons and my sign convention in Eq. (29) corresponds to $\Delta\Gamma_K > 0$. The Standard-Model prediction for $\Delta\Gamma_{B_d}$ and $\Delta\Gamma_{B_s}$ is also positive, while no reliable prediction is possible for the sign of $\Delta\Gamma_D$. The matrix appearing in Eq. (28) can be compactly written as

$$Q \begin{pmatrix} e^{-iM_L t - \Gamma_L t/2} & 0 \\ 0 & e^{-iM_H t - \Gamma_H t/2} \end{pmatrix} Q^{-1} \;=\; \begin{pmatrix} g_+(t) & \dfrac{q}{p} g_-(t) \\ \dfrac{p}{q} g_-(t) & g_+(t) \end{pmatrix} \tag{30}$$

with

$$\begin{aligned} g_+(t) &= e^{-imt}\, e^{-\Gamma t/2} \left[\cosh\frac{\Delta\Gamma\, t}{4}\, \cos\frac{\Delta M\, t}{2} - i \sinh\frac{\Delta\Gamma\, t}{4}\, \sin\frac{\Delta M\, t}{2} \right], \\ g_-(t) &= e^{-imt}\, e^{-\Gamma t/2} \left[-\sinh\frac{\Delta\Gamma\, t}{4}\, \cos\frac{\Delta M\, t}{2} + i \cosh\frac{\Delta\Gamma\, t}{4}\, \sin\frac{\Delta M\, t}{2} \right]. \end{aligned} \tag{31}$$

Inserting Eq. (30) into Eq. (28) gives us a transparent picture of the meson-antimeson oscillations:

$$\begin{aligned} |M(t)\rangle &= g_+(t)\, |M\rangle + \frac{q}{p}\, g_-(t)\, |\overline{M}\rangle\,, \\ |\overline{M}(t)\rangle &= \frac{p}{q}\, g_-(t)\, |M\rangle + g_+(t)\, |\overline{M}\rangle\,, \end{aligned} \tag{32}$$

We verify $g_+(0) = 1$ and $g_-(0) = 0$ and find that $g_\pm(t)$ has no zeros for $t > 0$ if $\Delta\Gamma \neq 0$. Hence an initially produced M will never turn into a pure $\overline{M}$ or back into a pure M. We will frequently encounter the combinations

$$\begin{aligned} |g_\pm(t)|^2 &= \frac{e^{-\Gamma t}}{2} \left[\cosh\frac{\Delta\Gamma\, t}{2} \pm \cos\left(\Delta M\, t\right) \right], \\ g_+^*(t)\, g_-(t) &= \frac{e^{-\Gamma t}}{2} \left[-\sinh\frac{\Delta\Gamma\, t}{2} + i \sin\left(\Delta M\, t\right) \right]. \end{aligned} \tag{33}$$

2.2 ΔM, $\Delta\Gamma$ and CP violation in mixing

We still need to solve our eigenvalue problem. The secular equation for the two eigenvalues $\sigma_{L,H} = M_{L,H} - i\Gamma_{L,H}/2$ of Σ is $(\Sigma_{11} - \sigma_{L,H})^2 - \Sigma_{12}\Sigma_{21} = 0$. The two solutions of this equation therefore satisfy

$$(\sigma_H - \sigma_L)^2 = 4\, \Sigma_{12}\Sigma_{21}$$

or

$$(\Delta M + i\frac{\Delta\Gamma}{2})^2 = 4\left(M_{12} - i\frac{\Gamma_{12}}{2}\right)\left(M_{12}^* - i\frac{\Gamma_{12}^*}{2}\right). \tag{34}$$

Taking real and imaginary part of this equation leads us to

$$(\Delta M)^2 - \frac{1}{4}\,(\Delta\Gamma)^2 = 4\,|M_{12}|^2 - |\Gamma_{12}|^2\,, \tag{35}$$

$$\Delta M\, \Delta\Gamma = -4\, \mathrm{Re}\,(M_{12}\Gamma_{12}^*)\,, \tag{36}$$

Further Eq. (26) implies $[Q^{-1}\Sigma Q]_{12} = [Q^{-1}\Sigma Q]_{21} = 0$, which determines

$$\frac{q}{p} = -\frac{\Delta M + i\,\Delta\Gamma/2}{2M_{12} - i\,\Gamma_{12}} = -\frac{2M_{12}^* - i\,\Gamma_{12}^*}{\Delta M + i\,\Delta\Gamma/2}\,. \tag{37}$$

(There is also a second solution with the opposite sign, which, however, is eliminated by imposing $\Delta M > 0$.) For the simplification of Eqs. (35–37) it is useful to identify the physical quantities of the mixing problem in Eqs. (22) and (23). In quantum mechanics we can always multiply either $|M\rangle$ or

$|\overline{M}\rangle$ by an arbitrary phase factor without changing the physics. This will change the phases of M_{12}, Γ_{12} and q/p, none of which can therefore have any physical meaning. The three physical quantities of meson-antimeson mixing are

$$|M_{12}|, \qquad |\Gamma_{12}|, \qquad \text{and} \quad \phi = \arg\left(-\frac{M_{12}}{\Gamma_{12}}\right). \tag{38}$$

Eq. (36) then reads

$$\Delta M \, \Delta\Gamma = 4\,|M_{12}||\Gamma_{12}|\cos\phi. \tag{39}$$

We can easily solve Eqs. (35) and (39) to express ΔM and $\Delta\Gamma$, which we want to measure by studying meson time evolutions, in terms of the theoretical quantities $|M_{12}|$, $|\Gamma_{12}|$ and ϕ. We recognise that the phase ϕ is responsible for *CP* violation in mixing introduced after Eq. (17): By multiplying the two expression for q/p in Eq. (37) with each other we find

$$\left(\frac{q}{p}\right)^2 = \frac{2M_{12}^* - i\,\Gamma_{12}^*}{2M_{12} - i\,\Gamma_{12}} = \frac{M_{12}^*}{M_{12}} \frac{1 + i\left|\dfrac{\Gamma_{12}}{2M_{12}}\right| e^{i\phi}}{1 + i\left|\dfrac{\Gamma_{12}}{2M_{12}}\right| e^{-i\phi}}. \tag{40}$$

We immediately verify from this expression that $\phi \neq 0, \pi$ indeed implies $|q/p| \neq 1$, which defines *CP* violation in mixing.

Interestingly, *CP* violation in mixing is small (if quantified in terms of $|q/p| - 1$) for the K, B_d and B_s systems. For $D-\overline{D}$ mixing this is most likely also the case, but the experimental data are not accurate enough at present. In the case of $K-\overline{K}$ mixing we have established this phenomenon in Eq. (17) from the measured value of $\mathrm{Re}\,\epsilon_K$ in Eq. (16). In the $B-\overline{B}$ systems the line of arguments is as follows: Experimentally we know $\Delta M \gg \Delta\Gamma$ and theoretically $|\Gamma_{12}| \ll \Delta M$ is firmly established from a SM calculation, since the possible impact of new physics on $|\Gamma_{12}|$ is small. Then Eqs. (35) and (39) imply $\Delta M \approx 2|M_{12}|$ and therefore $|\Gamma_{12}| \ll |M_{12}|$, so that the second term in the numerator and denominator of Eq. (40) is small, irrespective of the value of ϕ. Thus $|q/p| \simeq 1$ for B_d and B_s mesons. It is useful to define the quantity a through

$$\left|\frac{q}{p}\right|^2 = 1 - a. \tag{41}$$

For the K, B_d and B_s systems we know that a is small. By expanding $(q/p)^2$ in Eq. (40) in terms of ϕ or Γ_{12}/M_{12} we find

$$a = \frac{4|\Gamma_{12}|\,|M_{12}|}{4|M_{12}|^2 + |\Gamma_{12}|^2}\,\phi + \mathcal{O}(\phi^2), \qquad \text{for } K-\overline{K} \text{ mixing} \tag{42}$$

$$a = \mathrm{Im}\,\frac{\Gamma_{12}}{M_{12}} + \mathcal{O}\left(\left(\mathrm{Im}\,\frac{\Gamma_{12}}{M_{12}}\right)^2\right) = \left|\frac{\Gamma_{12}}{M_{12}}\right| \sin\phi\,, \qquad \text{for } B-\overline{B} \text{ mixing.} \tag{43}$$

With this result it is straightforward to solve Eqs. (35) and (39) for ΔM and $\Delta\Gamma$. Incidentally, in both cases we have

$$\Delta M \simeq 2\,|M_{12}|, \tag{44}$$

$$\Delta\Gamma \simeq 2\,|\Gamma_{12}|\cos\phi. \tag{45}$$

which holds up to corrections of order ϕ^2 for Kaons and of order $|\Gamma_{12}/M_{12}|^2$ for B mesons. Of course, in the former case one can also replace $\cos\phi$ by 1. Importantly, in B physics one deduces from Eq. (37) that

$$\frac{q}{p} \quad = \quad -\frac{M_{12}^*}{|M_{12}|}\left[1+\mathcal{O}(a)\right]. \tag{46}$$

That is, the phase of $-q/p$ is essentially given by the phase of the $B_d-\overline{B}_d$ or $B_s-\overline{B}_s$ box diagram in Fig. 1. Since $B-\overline{B}$ mixing is dominated by the box diagram with internal tops we readily infer

$$\frac{q}{p} \quad = \quad -\frac{V_{tb}^* V_{tq}}{V_{tb} V_{tq}^*} \;=\; -\exp[i\arg{(V_{tb}^* V_{tq})^2}] \qquad\qquad \text{for } B_q-\overline{B}_q \text{ mixing with } q=d,s \tag{47}$$

up to tiny corrections of order a.

2.3 Time-dependent decay rates

Flavour factories are e^+e^- colliders whose CMS energy matches the mass of an excited quarkonium state which predominantly decays into $(M,\overline{M})$ pairs. Running on the $\psi(3770)$, $\Upsilon(4S)$ or $\Upsilon(5S)$ resonances, one copiously produces $(D,\overline{D})$, $(B_d,\overline{B}_d)$ or $(B_s,\overline{B}_s)$ mesons. The $(M,\overline{M})$ pairs are in an entangled quantum-mechanical state until the decay of one of the mesons is observed. If the decay mode $M\to f$ is allowed while $\overline{M}\to f$ is forbidden one calls $M\to f$ a *flavour-specific* mode or a *tagging mode*. The most prominent examples are the semileptonic decays $M\to X\ell^+\nu_\ell$. For the discovery of $B_s-\overline{B}_s$ mixing the flavour-specific mode $B_s\to D_s^-\pi^+$ has played an important role [14]. A flavour-specific decay tags the decaying meson as either M or $\overline{M}$. The Einstein-Podolsky-Rosen effect then ensures that the other meson is an $\overline{M}$ or M, respectively. The time of the flavour tagging "starts the clock", i.e. defines $t=0$ in Eqs. (31) and (32). This method is called *opposite-side tagging*. In hadron colliders pairs of different hadrons can be produced, e.g. a B_s can be produced together with a B^- or Λ_b plus several lighter hadrons. Still, at the quark level $(\overline{b},b)$ pairs are produced, so that the flavour tagging works as well. As an additional possibility, hadron colliders permit *same-side tagging*, where the flavour is determined at the time of the hadronisation process: When, say, a b-quark hadronises into a $\overline{B}$ meson several pions and Kaons are produced as well. The charges of these light mesons are correlated with the charge of the light valence quark, which in the case of the $\overline{B}$ meson is an anti-d quark.

The time-dependent decay rate of a meson tagged at $t=0$ as M is defined as

$$\Gamma(M(t)\to f) = \frac{1}{N_M}\,\frac{d\,N(M(t)\to f)}{d\,t}, \tag{48}$$

where $d\,N(M(t)\to f)$ denotes the number of decays into the final state f occurring within the time interval between t and $t+d\,t$. N_M is the total number of M's produced at time $t=0$. An analogous definition holds for $\Gamma(\overline{M}(t)\to f)$. One has

$$\Gamma(M(t)\to f) = \mathcal{N}_f\,|\langle f|S|M(t)\rangle|^2, \qquad \Gamma(\overline{M}(t)\to f) = \mathcal{N}_f\,\left|\langle f|S|\overline{M}(t)\rangle\right|^2 \tag{49}$$

with the time-independent normalisation factor $\mathcal{N}_f$ comprising the result of the phase-space integration. It is straightforward to calculate $\Gamma(M(t)\to f)$ and $\Gamma(\overline{M}(t)\to f)$ in terms of A_f and $\overline{A}_f$

defined in Eq. (12), we just need to insert $|M(t)\rangle$ and $|\overline{M}(t)\rangle$ from Eq. (32) into Eq. (49). Trading $\overline{A}_f$ for λ_f (see Eq. (13)) and a (see Eq. (41)) and making use of Eq. (33) we find the desired formulae:

$$\begin{aligned}\Gamma(M(t)\to f) &= \mathcal{N}_f\,|A_f|^2\,e^{-\Gamma t}\left\{\frac{1+|\lambda_f|^2}{2}\cosh\frac{\Delta\Gamma\,t}{2}+\frac{1-|\lambda_f|^2}{2}\cos(\Delta M\,t)\right.\\ &\qquad\left.-\mathrm{Re}\,\lambda_f\,\sinh\frac{\Delta\Gamma\,t}{2}-\mathrm{Im}\,\lambda_f\,\sin\left(\Delta M\,t\right)\right\}, \qquad (50)\\ \Gamma(\overline{M}(t)\to f) &= \mathcal{N}_f\,|A_f|^2\,\frac{1}{1-a}\,e^{-\Gamma t}\left\{\frac{1+|\lambda_f|^2}{2}\cosh\frac{\Delta\Gamma\,t}{2}-\frac{1-|\lambda_f|^2}{2}\cos(\Delta M\,t)\right.\\ &\qquad\left.-\mathrm{Re}\,\lambda_f\,\sinh\frac{\Delta\Gamma\,t}{2}+\mathrm{Im}\,\lambda_f\,\sin(\Delta M\,t)\right\}. \qquad (51)\end{aligned}$$

Often we want to compare these decay modes with the corresponding decays into the final state which is CP-conjugate with respect to f. For states f with two or more particles we define

$$|\overline{f}\rangle = CP\,|f\rangle\,, \qquad (52)$$

while for the initial one-particle states we have defined *CP* in Eq. (9). For example, for $f = D_s^-\pi^+$ the *CP*-conjugate state is $\overline{f} = D_s^+\pi^-$. Whenever we discuss *CP* (or any other discrete transformation) in decay processes, we apply the transformation in the rest frame of the decaying meson. The transformation in Eq. (52) is understood to reverse the signs of three-momenta as in Eq. (9). For two-body final states, which are our prime focus, we can rotate this mirror-reflected state by 180°, so that the three-momenta of the rotated *CP*-transformed state coincide with those of the original state. This procedure is usually implicitly understood when people discuss decays into *CP* eigenstates composed of two distinct particles, such as $K\to\pi^+\pi^-$. For a *CP* eigenstate f_{CP} Eqs. (10) and (52) imply $|\overline{f}_{\mathrm{CP}}\rangle = \eta_{f_{CP}}|f_{\mathrm{CP}}\rangle$.

In the $M(t)\to\overline{f}$ decay rates it is advantageous to keep $\overline{A}_{\overline{f}}$ while trading $A_{\overline{f}}$ for $\lambda_{\overline{f}}$:

$$\begin{aligned}\Gamma(M(t)\to\overline{f}) &= \mathcal{N}_f\left|\overline{A}_{\overline{f}}\right|^2 e^{-\Gamma t}\,(1-a)\left\{\frac{1+|\lambda_{\overline{f}}|^{-2}}{2}\cosh\frac{\Delta\Gamma\,t}{2}-\frac{1-|\lambda_{\overline{f}}|^{-2}}{2}\cos(\Delta M\,t)\right.\\ &\qquad\left.-\mathrm{Re}\,\frac{1}{\lambda_{\overline{f}}}\,\sinh\frac{\Delta\Gamma\,t}{2}+\mathrm{Im}\,\frac{1}{\lambda_{\overline{f}}}\,\sin(\Delta M\,t)\right\}, \qquad (53)\\ \Gamma(\overline{M}(t)\to\overline{f}) &= \mathcal{N}_f\left|\overline{A}_{\overline{f}}\right|^2 e^{-\Gamma t}\left\{\frac{1+|\lambda_{\overline{f}}|^{-2}}{2}\cosh\frac{\Delta\Gamma\,t}{2}+\frac{1-|\lambda_{\overline{f}}|^{-2}}{2}\cos(\Delta M\,t)\right.\\ &\qquad\left.-\mathrm{Re}\,\frac{1}{\lambda_{\overline{f}}}\,\sinh\frac{\Delta\Gamma\,t}{2}-\mathrm{Im}\,\frac{1}{\lambda_{\overline{f}}}\,\sin(\Delta M\,t)\right\}. \qquad (54)\end{aligned}$$

Eqs. (50–51) and Eqs. (53–54) are our master formulae to calculate any time-dependent decay rate of interest. We discuss two important applications here. The first one is the time dependence of a flavour-specific decay, which satisfies $\overline{A}_f = A_{\overline{f}} = \lambda_f = 1/\lambda_{\overline{f}} = 0$. In addition we consider a decay mode with $|\overline{A}_{\overline{f}}| = |A_f|$, that is without direct CP violation. Semileptonic decays satisfy both conditions. Our master formulae become very simple for this case. Defining the *mixing asymmetry*,

$$\mathcal{A}_0(t) = \frac{\Gamma(M(t) \to f) - \Gamma(M(t) \to \overline{f})}{\Gamma(M(t) \to f) + \Gamma(M(t) \to \overline{f})}, \tag{55}$$

one finds to order a:

$$\mathcal{A}_0(t) = \frac{\cos(\Delta M\, t)}{\cosh(\Delta\Gamma\, t/2)} + \frac{a}{2}\left[1 - \frac{\cos^2(\Delta M\, t)}{\cosh^2(\Delta\Gamma\, t/2)}\right]. \tag{56}$$

Note that $\mathcal{A}_0(t)$ is not a *CP* asymmetry. Instead $\Gamma(M(t) \to f) \propto |\langle M|M(t)\rangle|^2$ is proportional to the probability that an "unmixed" M decays to f at time t, while $\Gamma(M(t) \to \overline{f}) \propto |\langle \overline{M}|M(t)\rangle|^2$ is the corresponding probability for the process $M \to \overline{M} \to f$. The asymmetry $\mathcal{A}_0(t)$ is often employed to measure ΔM. In the ARGUS discovery of B_d–$\overline{B}_d$ mixing [7] no time-dependence was observed. Instead so-called like-sign dilepton events were observed in semileptonic $(B_d, \overline{B}_d)$ decays, meaning that one of the two mesons must have mixed. By counting these events and comparing the number with the number of opposite-sign dilepton events one can infer the quantity $x = \Delta M/\Gamma$. The corresponding formula can be found by integrating our master formulae over t.

The *CP asymmetry in flavour-specific decays* (often called *semileptonic CP asymmetry*) reads

$$a_{\rm fs} \equiv \frac{\Gamma(\overline{M}(t) \to f) - \Gamma(M(t) \to \overline{f})}{\Gamma(\overline{M}(t) \to f) + \Gamma(M(t) \to \overline{f})} = \frac{1-(1-a)^2}{1+(1-a)^2} = a + \mathcal{O}(a^2). \tag{57}$$

Define the untagged decay rate

$$\Gamma[f,t] = \Gamma(\overline{M}(t) \to f) + \Gamma(M(t) \to f) \tag{58}$$

to find:

$$a_{\rm fs,unt}(t) = \frac{\Gamma[f,t] - \Gamma[\overline{f},t]}{\Gamma[f,t] + \Gamma[\overline{f},t]} = \frac{a_{\rm fs}}{2} - \frac{a_{\rm fs}}{2}\frac{\cos(\Delta M\, t)}{\cosh(\Delta\Gamma t/2)}. \tag{59}$$

Hence no tagging is needed to measure $a_{\rm fs}$! We observe that we can determine the three physical quantities characterising meson-antimeson mixing, $|M_{12}|$, $|\Gamma_{12}|$ and a, by measuring ΔM, $\Delta\Gamma$ and $a_{\rm fs}$. At present all three quantities are only measured for $K-\overline{K}$ mixing! Also the semileptonic *CP* asymmetry of B mesons can be measured without observing any time dependence. In the spirit of ARGUS we can compare the number of positively-charged like-sign dilepton pairs with the number of negatively-charged ones. Such measurements are performed at the B factories and the Tevatron, but no non-zero semileptonic *CP* asymmetry has been established by now.

Amusingly, the oscillations drop out from the tagged quantity in Eq. (57), while they persist in Eq. (59). In most applications one can neglect the tiny a in Eqs. (50–51) and Eqs. (53–54). Then we realise that in the untagged rates, obtained by adding Eqs. (50) and (51) or Eqs. (53) and (54), the terms involving $\cos(\Delta M t)$ and $\sin(\Delta M t)$ vanish.

The second application of our master formulae are decays into CP eigenstates, $M \to f_{\rm CP}$. The time-dependent *CP* asymmetry is

$$a_{f_{\rm CP}}(t) = \frac{\Gamma(\overline{M}(t) \to f_{\rm CP}) - \Gamma(M(t) \to f_{\rm CP})}{\Gamma(\overline{M}(t) \to f_{\rm CP}) + \Gamma(M(t) \to f_{\rm CP})}. \tag{60}$$

Using Eq. (50) and Eq. (51) one finds

$$a_{f_{\rm CP}}(t) = -\frac{A_{CP}^{\rm dir}\cos(\Delta M\, t) + A_{CP}^{\rm mix}\sin(\Delta M\, t)}{\cosh(\Delta\Gamma\, t/2) + A_{\Delta\Gamma}\sinh(\Delta\Gamma\, t/2)} + \mathcal{O}(a)\,, \tag{61}$$

with (for $f = f_{\rm CP}$)

$$A_{CP}^{\rm dir} = \frac{1-|\lambda_f|^2}{1+|\lambda_f|^2}\,, \qquad A_{CP}^{\rm mix} = -\frac{2\,{\rm Im}\,\lambda_f}{1+|\lambda_f|^2}\,, \qquad A_{\Delta\Gamma} = -\frac{2\,{\rm Re}\,\lambda_f}{1+|\lambda_f|^2}. \tag{62}$$

Note that $|A_{CP}^{\rm dir}|^2 + |A_{CP}^{\rm mix}|^2 + |A_{\Delta\Gamma}|^2 = 1$. Experimentally one can track the time-dependence of $a_f(t)$ and read off the coefficients of $\cos(\Delta M\, t)$ and $\sin(\Delta M\, t)$, so that one can determine $|\lambda_f|$ and ${\rm Im}\,\lambda_f$. When studying decay amplitudes we can treat the weak interaction perturbatively by drawing quark-level Feynman diagrams involving the exchange of W-bosons. While we cannot fully compute those diagrams, because we cannot estimate how the quarks are "dressed" by the strong interaction, we can still assess the CP-violating phases by identifying the CKM elements in the diagrams. Decays in which all contributing Feynman diagrams carry the same CP-violating phase are called *golden modes*. These modes satisfy $|A_f| = |\overline{A}_{\overline{f}}|$, so that there is no direct CP violation. In a golden $M \to f_{\rm CP}$ decay this means $|\lambda_{f_{\rm CP}}| = 1$ and in Eqs. (61) and (62) we have $A_{CP}^{\rm dir} = 0$ and

$$A_{CP}^{\rm mix} = {\rm Im}\,\lambda_{f_{\rm CP}}. \tag{63}$$

Moreover the phase of $\overline{A}_{f_{\rm CP}}/A_{f_{\rm CP}}$ is trivially read off from the phase of the CKM elements. In B physics, where we also know the phase of q/p from Eq. (47), we can therefore directly relate the measured ${\rm Im}\,\lambda_{f_{\rm CP}}$ to phases of CKM elements, if $M \to f_{\rm CP}$ is golden.

3 Third lecture: Linking quarks to mesons

3.1 The Cabibbo-Kobayashi-Maskawa matrix

We have encountered the CKM matrix V in Eq. (3). A unitary 3×3 matrix can be parameterised by three angles and six complex phases. With the rephasings in Eqs. (7) and (8) we can eliminate five phases from V leaving us with one physical CP-violating phase. In the parameterisation favoured by the Particle Data Book one has

$$V = \begin{pmatrix} c_{12}c_{13} & s_{12}c_{13} & s_{13}e^{-i\delta_{13}} \\ -s_{12}c_{23} - c_{12}s_{23}s_{13}e^{i\delta_{13}} & c_{12}c_{23} - s_{12}s_{23}s_{13}e^{i\delta_{13}} & s_{23}c_{13} \\ s_{12}s_{23} - c_{12}c_{23}s_{13}e^{i\delta_{13}} & -c_{12}s_{23} - s_{12}c_{23}s_{13}e^{i\delta_{13}} & c_{23}c_{13} \end{pmatrix}, \tag{64}$$

where $c_{ij} = \cos\theta_{ij}$ and $s_{ij} = \sin\theta_{ij}$. The real angles θ_{ij} may be chosen so that $0 \le \theta_{ij} \le \pi/2$, and the phase δ_{13} so that $-\pi < \delta_{13} \le \pi$. For the discussion of CKM metrology it is useful to introduce the Wolfenstein parameterisation [15]

$$V = \begin{pmatrix} 1-\frac{1}{2}\lambda^2 & \lambda & A\lambda^3(\rho - i\eta) \\ -\lambda & 1-\frac{1}{2}\lambda^2 & A\lambda^2 \\ A\lambda^3(1-\rho-i\eta) & -A\lambda^2 & 1 \end{pmatrix} + O(\lambda^4)\,, \tag{65}$$

which is an expansion in terms of the small parameter $\lambda = 0.22$. The remaining three parameters A, ρ and η are a bit smaller than 1. The Wolfenstein parameterisation nicely reveals the hierarchical structure of the CKM matrix, with diagonal elements of order 1 and smallest elements in the upper right and lower left corners. We can now understand why the prediction of m_c from ΔM_K in 1974 was successful: Any contribution involving the top quark (at that time unknown and unimagined by the authors of Ref. [3]) to the upper left diagram in Fig. 1 is highly suppressed by small CKM elements, since $|V_{td}V_{ts}| \simeq \lambda^5$, while $|V_{cd}V_{cs}| \simeq |V_{ud}V_{us}| \simeq \sin\theta_c \simeq \lambda$. Further the upper left 2×2 submatrix, the Cabibbo matrix, is almost unitary and involves only a single parameter, the Cabibbo angle θ_c with $V_{ud} \simeq V_{cs} \simeq \cos\theta_c$ and $V_{us} \simeq -V_{cd} \simeq \lambda$. Therefore the two new elements V_{cd} and V_{cs} predicted in Ref. [2] were completely fixed in terms of the known θ_c. In the Wolfenstein approximation only V_{ub} and V_{td} have a complex phase and CP violation is characterised by $\eta \neq 0$.

Any unitary 3×3 matrix satisfies

$$\begin{aligned} V_{1j}^* V_{1k} + V_{2j}^* V_{2k} + V_{3j}^* V_{3k} &= \delta_{jk} && (66)\\ \text{and} \qquad V_{j1}^* V_{k1} + V_{j2}^* V_{k2} + V_{j3}^* V_{k3} &= \delta_{jk}. && (67)\end{aligned}$$

If we choose $j \neq k$ the three terms add to zero. We can depict the relations in Eqs. (66) and (67) as triangles in the complex plane, e.g. for Eq. (66) the three corners are located at 0, $V_{1j}^* V_{1k}$ and $-V_{2j}^* V_{2k}$. The three sides can be associated with the three terms summing to zero. The area of all six triangles is the same and given by $J/2$, where J is the *Jarlskog invariant* [16]

$$J \equiv \mathrm{Im}\,[V_{td}^* V_{tb} V_{ub}^* V_{ud}] = c_{12}c_{23}c_{13}^2 s_{12}s_{23}s_{13}\sin\delta_{13} \simeq A^2\lambda^6\eta. \qquad (68)$$

Here the third expression refers to the exact parameterisation of Eq. (64) and the last result uses the Wolfenstein approximation. Four of the six *unitarity triangles* are squashed, the three sides are similar only for the choice $(j,k) = (3,1)$. Moreover, within the Wolfenstein approximation the shapes of the triangles corresponding to Eqs. (66) and (67) are equal for $(j,k) = (3,1)$. Applying the phase transformations of Eqs. (7) and (8) rotates the unitarity triangles in the complex plane, but leaves their shape fixed. Seeking a definition of a rephasing-invariant unitarity triangle with a physical meaning we divide Eq. (66) (for $(j,k) = (3,1)$) by $V_{23}^* V_{21} = V_{cb}^* V_{cd}$ to arrive at

$$\frac{V_{ub}^* V_{ud}}{V_{cb}^* V_{cd}} + \frac{V_{tb}^* V_{td}}{V_{cb}^* V_{cd}} + 1 = 0 \qquad (69)$$

When people speak of "the" unitarity triangle they refer to the rescaled triangle defined by Eq. (69). Since its baseline coincides with the interval $[0,1]$ of the real axis, the unitarity triangle is completely determined by the location of its apex $(\overline{\rho}, \overline{\eta})$, where

$$\overline{\rho} + i\overline{\eta} \equiv -\frac{V_{ub}^* V_{ud}}{V_{cb}^* V_{cd}}. \qquad (70)$$

Inserting Eq. (65) into Eq. (70) one realises that $(\overline{\rho}, \overline{\eta}) = (\rho, \eta)$ within the Wolfenstein approximation, which here is good to an accuracy of 3%. The unitarity triangle is depicted in Fig. 3. The two non-trivial sides of the triangle are

$$R_u \equiv \sqrt{\overline{\rho}^2 + \overline{\eta}^2}, \qquad R_t \equiv \sqrt{(1-\overline{\rho})^2 + \overline{\eta}^2}. \qquad (71)$$

CP-violating quantities are associated with the triangle's three angles

$$\alpha = \arg\left[-\frac{V_{td}V_{tb}^*}{V_{ud}V_{ub}^*}\right], \qquad \beta = \arg\left[-\frac{V_{cd}V_{cb}^*}{V_{td}V_{tb}^*}\right], \qquad \gamma = \arg\left[-\frac{V_{ud}V_{ub}^*}{V_{cd}V_{cb}^*}\right]. \qquad (72)$$

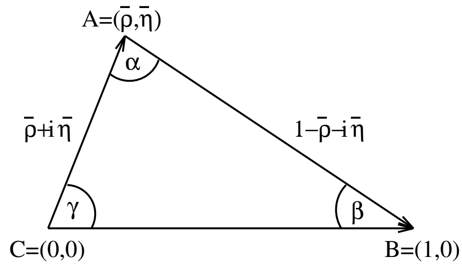

Figure 3: The (standard) unitarity triangle.

The angle γ coincides with δ_{13} of Eq. (64) at the sub-permille level. With Eqs. (70–72) one obtains

$$\overline{\rho} + i\overline{\eta} \;=\; R_u e^{i\gamma}, \qquad\qquad 1 - \overline{\rho} - i\overline{\eta} \;=\; R_t e^{-i\beta}. \tag{73}$$

The unitarity relation of Eq. (69) now simply reads

$$R_u e^{i\gamma} + R_t e^{-i\beta} \;=\; 1 \tag{74}$$

Taking real and imaginary parts of Eq. (74) reproduces formulae which you know from high-school geometry, allowing us to express any two of the four quantities R_u, R_t, γ, β in terms of the remaining two ones. By multiplying Eq. (74) with either $\exp(-i\gamma)$ or $\exp(i\beta)$ one finds analogous relations involving $\alpha = \pi - \beta - \gamma$.

Sometimes one needs to refine the Wolfenstein approximation to higher orders in λ. It is prudent to define [17]

$$\lambda \equiv s_{12}, \qquad\qquad A\lambda^2 \equiv s_{23} \tag{75}$$

to all orders in λ and to expand all CKM elements in terms of λ, A, $\overline{\rho}$ and $\overline{\eta}$ to the desired order in λ. Then, for example:

$$V_{ub} \;=\; A\lambda^3(\overline{\rho} - i\overline{\eta}) \left(1 + \frac{\lambda^2}{2} + \mathcal{O}(\lambda^4)\right). \tag{76}$$

The phase

$$\beta_s = \arg\left[-\frac{V_{ts}V_{tb}^*}{V_{cs}V_{cb}^*}\right] = \lambda^2\overline{\eta} + O(\lambda^4) \tag{77}$$

plays an important role in B_s–$\overline{B}_s$ mixing; β_s is small, of order 0.02 (equal to 1 degree). In the phase convention of Eq. (64) the phase of $V_{cs}V_{cb}^*$ is $\mathcal{O}(\lambda^6)$ and

$$\arg(-V_{ts}) = \beta_s(1 + O(\lambda^2)). \tag{78}$$

Organising the phases in powers of λ, we find all CKM elements real to order λ^2 except for V_{ub}, V_{td} and V_{ts}. Going to higher orders one encounters $\arg(-V_{cd}) \simeq A^2\overline{\eta}\lambda^4$ and $\arg(V_{cs}) \simeq -A^2\overline{\eta}\lambda^6$.

3.2 Effective Hamiltonians

We now address the strong interaction, which is the main obstacle on our way from quark diagrams to mesonic amplitudes like M_{12} and $A(M \to f)$. In Sect. 1.1 we have seen that weak processes of

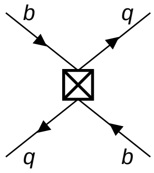

Figure 4: The four-quark operator Q for $B_q - \overline{B}_q$ mixing with $q = d$ or s.

mesons are multi-scale processes. For instance, $B-\overline{B}$ mixing involves three largely separated scales, since $m_t \sim M_W \gg m_b \gg \Lambda_{\rm QCD}$. These scales must be disentangled to separate the short-distance QCD, which is described by the exchange of quarks and gluons, from the long-distance hadronic physics, whose characteristic property is the confinement of quarks into hadrons. The key tool to separate the physics associated with the scale $m_{\rm heavy}$ from the dynamics associated with $m_{\rm light} \ll m_{\rm heavy}$ is the construction of an *effective field theory*. The corresponding *effective Hamiltonian* $H^{\rm eff}$ is designed to reproduce the S-matrix elements of the Standard Model up to corrections of order $(m_{\rm light}/m_{\rm heavy})^n$ where n is a positive integer:

$$\langle f|\mathbf{T}e^{-i\int d^4x H_{\rm int}^{\rm SM}(x)}|i\rangle \quad = \quad \langle f|\mathbf{T}e^{-i\int d^4x H^{\rm eff}(x)}|i\rangle \left[1 + \mathcal{O}\left(\frac{m_{\rm light}}{m_{\rm heavy}}\right)^n\right] \tag{79}$$

I exemplify the method with an effective Hamiltonian which reproduces the amplitude for $B-\overline{B}$ mixing up to corrections of order m_b^2/M_W^2. That is, we employ Eq. (79) for the case $i = \overline{B}$ and $f = B$ (where $B = B_d$ or B_s), $m_{\rm light} = m_b$ and $m_{\rm heavy} = M_W \sim m_t$. The corresponding effective Hamiltonian reads

$$H^{\rm eff} \quad = \quad H^{\rm QCD(f=5)} + H^{\rm QED(f=5)} + H^{|\Delta B|=2}. \tag{80}$$

Here the first two terms are the usual QCD and QED interaction Hamiltonians with 5 "active flavours", meaning that they do not involve the top quark. The last term describes the weak interaction. Adapted to the process under study, $H^{|\Delta B|=2}$ only encodes the physics related to $B-\overline{B}$ mixing, but does not describe other weak processes such as meson decays. It is called $H^{|\Delta B|=2}$, because it describes physical processes in which the bottom quantum number B changes by two units. $H^{|\Delta B|=2}$ does not contain W-boson, Z-boson or top-quark fields, instead the $\Delta B = 2$ transition of the box diagram in Fig. 1 is mediated by an effective four-quark coupling:

$$Q \quad = \quad \overline{q}_L \gamma_\nu b_L \, \overline{q}_L \gamma^\nu b_L \qquad\qquad \text{with } q = d \text{ or } s. \tag{81}$$

For historical reasons Q is called a *four-quark operator*, but it is nothing but a point-like coupling of four quark fields as shown in Fig. 4. We have

$$H^{|\Delta B|=2} = \frac{G_F^2}{4\pi^2} \, (V_{tb}V_{tq}^*)^2 \, C^{|\Delta B|=2}(m_t, M_W, \mu) \, Q(\mu) + h.c. \tag{82}$$

where the lengthy expression multiplying Q is just the effective coupling constant multiplying the four-quark interaction of Fig. 4. This coupling constant is split into several factors, the first of which contains the Fermi constant G_F. The second factor summarises the CKM elements of the box diagram and the third factor $C^{|\Delta B|=2}(m_t, M_W, \mu)$ is the *Wilson coefficient*, which contains the information on the heavy mass scales M_W and m_t. Finally μ is the renormalisation scale, familiar from QCD. Just as any other coupling also Q must be renormalised. The renormalised operator Q depends on μ through the renormalisation constant $Z_Q(\mu)$ via $Q = Z_Q Q^{\rm bare}$ and (in a mass-independent scheme like $\overline{\rm MS}$) the latter dependence is only implicit through $g(\mu)$, where g is the QCD coupling constant.[4] With the decomposition in Eq. (82) $C^{|\Delta B|=2}$ has dimension two and is real.

$C^{|\Delta B|=2}$ is calculated from the defining property of $H^{\rm eff}$ in Eq. (79): We compute the $\Delta B = 2$ process both in the Standard Model and with the interactions of $H^{\rm eff}$ and adjust $C^{|\Delta B|=2}$ such that the two results are the same, up to corrections of order m_b^2/M_W^2. Obviously we cannot do this with mesons as external states i and f. But a crucial property of $H^{\rm eff}$ is the independence of the Wilson coefficient on the external states. We can compute it for an arbitrary momentum configuration for the external quarks as long as the external momenta are of the order of $m_{\rm light}$. That is, we do not need to know the complicated momentum configuration of quarks bound in a meson state. Further all QCD effects in $C^{|\Delta B|=2}$ are purely perturbative:

$$C^{|\Delta B|=2} \;=\; C^{|\Delta B|=2,(0)} + \frac{\alpha_s(\mu)}{4\pi} C^{|\Delta B|=2,(1)} + \ldots \tag{83}$$

We can understand why and how this works if we expand the result of the box diagram of Fig. 1 in terms of the momenta of the external quarks, which are at most of order m_b. The leading term consists of the result of a loop integral with external momenta set to zero and the spinors of the external quark states. Now the "effective theory side" of Eq. (79) involves the tree-level diagram corresponding to

$$\begin{aligned}\langle f|\mathbf{T} e^{-i\int d^4x H^{\rm eff}(x)}|i\rangle^{(0)} \;&\simeq\; -i\int d^4x \langle f|H^{\rm eff}(x)|i\rangle^{(0)} \;=\; -i\int d^4x \langle f|H^{|\Delta B|=2}(x)|i\rangle^{(0)} \\ &=\; -i(2\pi)^4\delta^{(4)}(p_f-p_i)\,\frac{G_F^2}{4\pi^2}\,(V_{tb}V_{tq}^*)^2\, C^{|\Delta B|=2,(0)}\,\langle f|Q|i\rangle^{(0)}\end{aligned}$$

where $|i\rangle = |p_b, s_b; p_{\overline{q}}, s_{\overline{q}}\rangle$ and $|f\rangle = |p_q, s_q; p_{\overline{b}}, s_{\overline{b}}\rangle$ are the external states characterised by the momenta and spins of the quarks. The superscript "(0)" indicates the lowest order of QCD everywhere. Since $\langle f|Q|i\rangle$ reproduces the spinor structure ("Dirac algebra") of the box diagram, the coefficient $C^{|\Delta B|=2,(0)}$ inferred from this *matching calculation* is solely determined in terms of the loop integral and therefore only depends on M_W and m_t. The matching calculation becomes less trivial when we go to the *next-to-leading order (NLO)* of QCD. Now $H^{\rm QCD}$ enters the matching calculation and we must dress both the box diagram and the effective diagram in Fig. 4 with gluons in all possible ways. Denoting the SM amplitude by

$$\mathcal{M} \;=\; \mathcal{M}^{(0)} + \frac{\alpha_s}{4\pi}\mathcal{M}^{(1)} + \ldots, \tag{84}$$

our NLO matching calculation amounts to the determination of $C^{|\Delta B|=2,(1)}$ from

$$\begin{aligned}-\mathcal{M}^{(0)} - \frac{\alpha_s}{4\pi}\mathcal{M}^{(1)} \;&=\; \frac{G_F^2}{4\pi^2}\,(V_{tb}V_{tq}^*)^2\,\left[C^{|\Delta B|=2,(0)} + \frac{\alpha_s}{4\pi}C^{|\Delta B|=2,(1)}\right] \\ &\quad\cdot\left[\langle Q\rangle^{(0)} + \frac{\alpha_s}{4\pi}\langle Q\rangle^{(1)}\right]\left[1+\mathcal{O}\left(\frac{m_b^2}{M_W^2}\right)\right] \;+\; \mathcal{O}\left(\alpha_s^2\right)\end{aligned} \tag{85}$$

On the RHS the external states are suppressed for simplicity of notation. The QCD corrections to the box diagram in $\mathcal{M}^{(1)}$ not only depend on the light scales, i.e. external momenta and light quark

[4] The analogy with the renormalisation of the QCD coupling constant is more obvious if one reads the product $CZ_QQ^{\rm bare}$ in a different way: By assigning Z_Q to C rather than Q one may view C as a renormalised coupling constant. The notion of a "renormalised" operator instead of a "renormalised Wilson coefficient" has historical reasons.

masses, they also suffer from infrared (IR) divergences. These divergences signal the breakdown of QCD perturbation theory at low energies. However, the gluonic corrections to Fig. 4, which are comprised in $\langle Q\rangle^{(1)}$, exactly reproduce the infrared structure of the SM diagrams: They involve the same IR divergences and have the same dependence on the light mass scales. Collecting the $\mathcal{O}(\alpha_s)$ terms from Eq. (85),

$$-\mathcal{M}^{(1)} = \frac{G_F^2}{4\pi^2}\,(V_{tb}V_{tq}^*)^2\,\left[C^{|\Delta B|=2,(0)}\langle Q\rangle^{(1)} + C^{|\Delta B|=2,(1)}\langle Q\rangle^{(0)}\right], \tag{86}$$

one finds identical IR structures on the LHS and in the first term in the square brackets, while $C^{|\Delta B|=2,(1)}$ only contains heavy masses and no IR divergences. In conclusion, the IR structure of the SM amplitude properly factorises with an "infrared-safe" $C^{|\Delta B|=2}$. This success can be understood by separately discussing the regions of small and large loop momentum passing through a gluon line in the diagrams of $\mathcal{M}^{(1)}$. The infrared-sensitive diagrams are identified as those in which the gluon connects two external quark lines. (The other diagrams are infrared-finite and one can set the light mass parameters to zero.) If the loop momentum traversing the gluon line is small, we can neglect it in the heavy top and W propagators. Therefore the loop integration factorises into two one-loop integrations and the second loop integral involving the heavy particles simply reproduces the one-loop result contained in $C^{|\Delta B|=2,(0)}$. The gluon-loop integration —still over soft momenta only— is equal to the one in the corresponding diagram in $\langle Q\rangle^{(1)}$, where the gluon connects the same quark lines. Therefore the region of integration with a soft gluon factorises with the leading-order coefficient $C^{|\Delta B|=2,(0)}$ in Eq. (85). The region of the momentum integration with a hard gluon momentum does not factorise in this way and contributes to $C^{|\Delta B|=2,(1)}$. However, the region of large gluon loop momentum is not infrared-sensitive and we can neglect the light momenta and masses. Therefore $C^{|\Delta B|=2,(1)}$ does not depend on the light mass scales. Conversely, $\langle Q\rangle$ contains only small scales of order $m_{\rm light}$ and encodes the full infrared structure of $\mathcal{M}$. Therefore our quark-level calculation is meaningful for $C^{|\Delta B|=2}$, but not for $\langle Q\rangle$. In order to make a theoretical prediction for the $B-\overline{B}$ mixing amplitude, we must compute $\langle B|Q|\overline{B}\rangle$ with nonperturbative methods. The factorisation of $\mathcal{M}$ into short-distance coefficients and long-distance operator matrix elements is also called *operator product expansion*.

Here I only derive the result for the leading-order (LO) Wilson coefficient $C^{|\Delta B|=2,(0)}$. In a first step let us decompose $\mathcal{M}^{(0)}$ as

$$\mathcal{M}^{(0)} = \sum_{j,k=u,c,t} V_{jb}^*V_{jq}\,V_{kb}^*V_{kq}\,\mathcal{M}_{jk}^{(0)}\,\langle Q\rangle^{(0)}, \qquad q=d \text{ or } s, \tag{87}$$

where $\mathcal{M}_{jk}^{(0)}\,\langle Q\rangle^{(0)}$ is the result of the box diagram containing internal quark flavours (j,k) with the CKM elements factored out. We then write

$$\mathcal{M}_{jk}^{(0)} = -\frac{G_F^2}{4\pi^2}\,M_W^2\,\widetilde{S}(x_j,x_k) \tag{88}$$

with $x_j = m_j^2/M_W^2$. The function $\widetilde{S}(x_j,x_k)$ is symmetric, $\widetilde{S}(x_j,x_k)=\widetilde{S}(x_k,x_j)$. In the next step we use CKM unitarity to eliminate $V_{ub}^*V_{uq} = -V_{tb}^*V_{tq} - V_{cb}^*V_{cq}$ from Eq. (87):

$$-\mathcal{M}^{(0)} = \frac{G_F^2}{4\pi^2}\,M_W^2\,\left[(V_{tb}^*V_{tq})^2\,S(x_t) + 2V_{tb}^*V_{tq}\,V_{cb}^*V_{cq}S(x_c,x_t) + (V_{cb}^*V_{cq})^2\,S(x_c)\right]\,\langle Q\rangle^{(0)}. \tag{89}$$

S and $\widetilde{S}$ are related as

$$\begin{aligned} S(x_j,x_k) &= \widetilde{S}(x_j,x_k) - \widetilde{S}(x_j,0) - \widetilde{S}(0,x_k) + \widetilde{S}(0,0), \qquad \text{for } j,k=c,t, \\ S(x) &\equiv S(x,x), \end{aligned} \tag{90}$$

where I have set the up-quark mass to zero. In Eq. (89) the last two terms are tiny, because $x_c \sim 10^{-4}$ and

$$S(x_c) = \mathcal{O}(x_c), \qquad S(x_c, x_t) = \mathcal{O}(x_c \ln x_c). \tag{91}$$

This consequence of CKM unitarity is called the *Glashow-Iliopoulos-Maiani (GIM)* suppression, related to the vanishing of FCNCs in the limit of equal internal quark masses (here m_c and $m_u = 0$). No GIM suppression occurs in top loops, because $x_t \sim 4$. The dominant contribution to Eq. (87) involves

$$S(x_t) \;=\; x_t \left[\frac{1}{4} + \frac{9}{4}\frac{1}{1-x_t} - \frac{3}{2}\frac{1}{(1-x_t)^2}\right] - \frac{3}{2}\left[\frac{x_t}{1-x_t}\right]^3 \ln x_t \;\approx\; 2.3. \tag{92}$$

The tiny charm contribution does not contribute to $C^{|\Delta B|=2,(0)}$ at all; to accommodate for it we must refine our operator product expansion to include higher powers of $(m_{\text{light}}/m_{\text{heavy}})$ in Eq. (79). We can read off $C^{|\Delta B|=2,(0)}$ from Eqs. (85) and (89):

$$C^{|\Delta B|=2,(0)}(m_t, M_W, \mu) = M_W^2\, S\,(x_t). \tag{93}$$

The functions $S(x)$ and $S(x_c, x_t)$ are called *Inami-Lim* functions [28].

The factorisation in Eqs. (79) and (85) also solves another problem: No largely separated scales appear in $C^{|\Delta B|=2}(m_t, M_W, \mu)$ provided that we take $\mu = \mathcal{O}(M_W, m_t)$, so that no large logarithms can spoil the convergence of the perturbative series. While no explicit μ-dependence is present in our LO result in Eq. (93), there is an implicit μ-dependence through $m_t(\mu)$, which is a running quark mass (typically defined in the $\overline{\text{MS}}$ scheme). $C^{|\Delta B|=2,(1)}$ also contains an explicit $\ln(\mu/M_W)$ term. Two sources contribute to this term: First, there is already a $\ln(\mu/M_W)$ term in $\mathcal{M}^{(1)}$, familiar to us from matrix elements with $\overline{\text{MS}}$-renormalised UV divergences. Second, $\mathcal{M}^{(1)}$ contains the large logarithm $\ln(m_b/M_W)$ which is split between matrix elements and Wilson coefficients as

$$\ln\frac{m_b}{M_W} \;=\; \ln\frac{m_b}{\mu} + \ln\frac{\mu}{M_W}. \tag{94}$$

This feature is transparent from Eq. (86).

The scale $\mu_{tW} = \mathcal{O}(M_W, m_t)$ at which we invoke Eq. (85) to find $C^{|\Delta B|=2}$ is called the *matching scale* and $C^{|\Delta B|=2}(m_t, M_W, \mu_{tW})$ has a good perturbative behaviour. Similarly, no large logarithms occur in $\langle Q(\mu_b)\rangle$, if we choose a scale $\mu_b \sim m_b$ in the matrix element. Since the μ-dependence in $H^{|\Delta B|=2}$ is spurious, we can take any value of μ we want, but this value must be the same in $C(\mu)$ and $\langle Q(\mu)\rangle$. That forces us to either relate $C(\mu_{tW})$ to $C(\mu_b)$ or to express $\langle Q(\mu_b)\rangle$ in terms of $\langle Q(\mu_{tW})\rangle$ in such a way that large logarithms

$$\alpha_s^n \ln^n \frac{\mu_{tW}}{\mu_b} \tag{95}$$

are summed to all orders $n = 0, 1, 2\ldots$ in perturbation theory. This can be achieved by solving the *renormalisation group (RG) equation* for either $C(\mu)$ or $\langle Q(\mu)\rangle$. All steps of this procedure are analogous to the calculation of the running quark mass, which can be found in any textbook on QCD. RG-improvement promotes our LO result to a *leading-log (LL)* quantity:

$$C^{|\Delta B|=2,(0)}(m_t, M_W, \mu_b) \;=\; u^{(0)}(\mu_b, \mu_{tW})C^{|\Delta B|=2,(0)}(m_t, M_W, \mu_{tW}) \tag{96}$$

$$\langle Q(\mu_{tW})\rangle \;=\; u^{(0)}(\mu_b, \mu_{tW})\langle Q(\mu_b)\rangle \tag{97}$$

$$u^{(0)}(\mu_b, \mu_{tW}) \;=\; \left(\frac{\alpha_s(\mu_{tW})}{\alpha_s(\mu_b)}\right)^{\frac{\gamma_+^{(0)}}{2\beta_0^{(5)}}} \qquad \text{with } \gamma_+^{(0)} = 4. \tag{98}$$

The evolution factor $u^{(0)}(\mu_b, \mu_{tW})$ depends on the *anomalous dimension* of Q, which equals $(\alpha_s/(4\pi))\gamma_+^{(0)}$ to LL accuracy. $\beta_0^{(f)} = 11 - 2f/3$ is the first term of the QCD β function. One usually writes

$$C^{|\Delta B|=2}(m_t, M_W, \mu_b) \quad = \quad \eta_B b_B(\mu_b) C^{|\Delta B|=2,(0)}(m_t, M_W, \mu_{tW}) \tag{99}$$

where all dependence on μ_b is absorbed into $b_B(\mu_b)$ and all heavy scales reside in η_B. This factorisation is possible to all orders in α_s. It is trivially verified in the LL approximation of Eq. (98), where simply $u^{(0)}(\mu_b, \mu_{tW}) = \eta_B b_B(\mu_b)$. In Eq. (99) m_t is understood as $m_t(m_t)$ (and not as $m_t(\mu_{tW})$). In this way η_B is independent of μ_{tW} to the calculated order; the residual μ_{tW} dependence is already tiny in the NLL result. η_B mildly depends on $x_t = m_t^2/M_W^2$ and in practice one can treat it as a constant number [18]:

$$\eta_B = 0.55, \qquad\qquad b_B(\mu_b = m_b = 4.2\,\text{GeV}) = 1.5. \tag{100}$$

The dependences of b_B on μ_b and the chosen renormalisation scheme cancel in the product $b_B(\mu_b)\langle Q(\mu_b)\rangle$. The quoted number is for the $\overline{\text{MS}}$–NDR scheme, where "NDR" refers to the treatment of the Dirac matrix γ_5. Details on this topic can be found in [19]. We see that the impact of short-distance QCD corrections is moderate, since $\eta_B\, b_B(\mu_b) = 0.84$. The NLL calculation of Ref. [18] has found only small two-loop corrections and the remaining uncertainty affects η_B only in the third digit behind the decimal point. RG-improved perturbation theory works superbly! Combining Eqs. (82), (93) and (99) we obtain our final expression for the $|\Delta B| = 2$ hamiltonian:

$$H^{|\Delta B|=2} \quad = \quad \frac{G_F^2}{4\pi^2}\, M_W^2\, (V_{tb}V_{tq}^*)^2\, \eta_B\, S(x_t) b_B(\mu_b) Q(\mu_b) \; + \; h.c. \tag{101}$$

Finally we cannot escape from quark confinement! Our hadronic matrix element is conventionally parameterised as

$$\langle B_q|Q(\mu_b)|\overline{B}_q\rangle \quad = \quad \frac{2}{3} M_{B_q}^2\, f_{B_q}^2\, \frac{\widehat{B}_{B_q}}{b_B(\mu_b)} \tag{102}$$

with the B_q meson decay constant f_{B_q} and the *bag factor* $\widehat{B}_{B_q}$. The parameterisation in Eq. (102) is chosen in such a way that $\widehat{B}_{B_q}/b_B(\mu_b)$ is close to one. It will be especially useful once precise experimental data on $f_{B_d} \sim f_{B^+}$ from leptonic B^+ decays will be available. With the help of our effective field theory we have beaten the problem of long-distance QCD in $B-\overline{B}$ mixing down to the calculation of a single number. Lattice gauge theory computations cover the ranges [29]

$$f_{B_d}\sqrt{\widehat{B}_{B_d}} \quad = \quad (225 \pm 35)\,\text{MeV}, \qquad\qquad f_{B_s}\sqrt{\widehat{B}_{B_s}} \; = \; (270 \pm 45)\,\text{MeV}. \tag{103}$$

The quoted hadronic uncertainties are the main problem in the extraction of $|V_{tb}V_{tq}|$ from the measured ΔM_{B_q}. $\widehat{B}_{B_d}$ could differ from $\widehat{B}_{B_s}$, but no computation has established any significant difference by now.

Putting Eqs. (101) and (102) together we find the desired element of the $B-\overline{B}$ mass matrix:

$$\begin{aligned} M_{12} \quad &= \quad \frac{\langle B_q|H^{|\Delta B|=2}|\overline{B}_q\rangle}{2M_{B_q}} \\ &= \quad \frac{G_F^2}{12\pi^2}\, \eta_B\, M_{B_q}\, \widehat{B}_{B_q} f_{B_q}^2\, M_W^2\, S\!\left(\frac{m_t^2}{M_W^2}\right) \left(V_{tb}V_{tq}^*\right)^2 . \end{aligned} \tag{104}$$

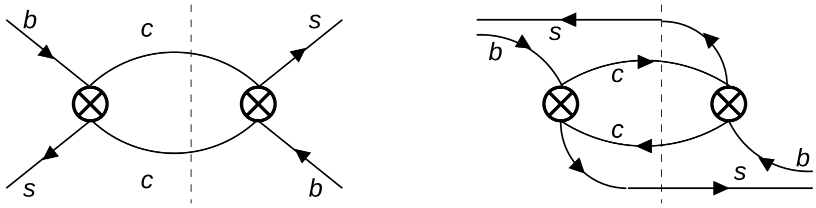

Figure 5: Second-order contribution of $H^{|\Delta B|=1}$ to $B_s - \overline{B}_s$ mixing. The diagrams constitute the dominant contribution to $\Delta\Gamma_{B_s}$.

We remark that there is no contribution of $H^{|\Delta B|=2}$ to Γ_{12}, because $\langle B_q|H^{|\Delta B|=2}|\overline{B}_q\rangle$ has no absorptive part. By inspecting Eq. (24) we can verify that the dispersive or absorptive part of some amplitude can be calculated by replacing the loop integrals by their real or imaginary parts, respectively, while keeping all complex CKM elements. But only diagrams with light internal quarks involve loop integrals with a non-zero imaginary part. Hence we must extend our effective-Hamiltonian formalism to include the effects of light internal quarks in the box diagrams, if we want to predict $\Delta\Gamma_{B_q}$. Contracting the heavy W-boson lines in the diagrams of Fig. 1 to a point does not correspond to a contribution from $H^{|\Delta B|=2}$ in the effective theory. Instead this is a second-order effect involving some effective $|\Delta B| = 1$-Hamiltonian $H^{|\Delta B|=1}$, which we must add to H^{eff} in Eq. (80). The relevant piece from the RHS of Eq. (79) is

$$-\frac{1}{2}\int d^4x d^4y \; \langle B|\mathbf{T}H^{|\Delta B|=1}(x)H^{|\Delta B|=1}(y)|\overline{B}\rangle. \tag{105}$$

The LO contribution to this bilocal matrix element is depicted in Fig. 5 for the case of $B_s - \overline{B}_s$ mixing. The contribution from Eq. (105) to $B - \overline{B}$ mixing is much smaller than the one from $H^{|\Delta B|=2}$, which is enhanced due to the heavy top mass entering Eq. (92). Therefore we can neglect the bilocal contribution in M_{12} and only need to consider it for Γ_{12}. From this observation we also conclude that $|\Gamma_{12}| \ll |M_{12}|$ leading to $|\Delta\Gamma| \ll \Delta M$, which we already exploited in Eqs. (43–47).

3.3 SM predictions of ΔM, $\Delta\Gamma$ and a_{fs}

In Sec. 3.2 we have collected all ingredients of the SM calculation of $\Delta M = 2|M_{12}|$ for the B_d and B_s systems. Looking at Eq. (65) we realise that $|V_{tb}|$ is well-known and $|V_{ts}|$ is essentially fixed by the well-measured $|V_{cb}|$. From Eqs. (104) and (103) we find the SM prediction

$$\Delta M_{B_s} = (12.5 \pm 4.3)\ \text{meV} = (19.0 \pm 6.6)\ \text{ps}^{-1}. \tag{106}$$

The first unit is milli-electronvolt, a unit which we do not encounter often in high-energy physics. By dividing with $\hbar$ one finds the second expression in terms of inverse picoseconds, which is more useful since ΔM is measured from the oscillation frequency in Eq. (55). Eq. (106) is in good agreement with the Tevatron measurement of [14,20]

$$\Delta M_{B_s}^{\text{exp}} = \left(17.77 \pm 0.10_{(\text{stat})} \pm 0.07_{(\text{syst})}\right)\ \text{ps}^{-1}. \tag{107}$$

The corresponding quantity for $B_d - \overline{B}_d$ mixing is well-measured by several experiments with [8]

$$\Delta M_{B_d}^{\text{exp}} = (333.7 \pm 3.3)\ \mu\text{eV} = (0.507 \pm 0.005)\ \text{ps}^{-1}. \tag{108}$$

We can use ΔM_{B_d} to determine $|V_{td}|$. From Eq. (104) we infer

$$\Delta M_{B_d} = (0.52 \pm 0.02)\,\text{ps}^{-1} \left(\frac{|V_{td}|}{0.0082} \right)^2 \left(\frac{f_{B_d}\sqrt{\widehat{B}_{B_d}}}{225\,\text{MeV}} \right)^2 . \tag{109}$$

The 16% error of the lattice value in Eq. (103) dominates the uncertainty on the extracted $|V_{td}|$. The all-order Wolfenstein parameterisation defined by Eqs. (70) and (75) implies

$$|V_{td}| = A\lambda^3 R_t + \mathcal{O}(\lambda^5). \tag{110}$$

Since $A\lambda^2 \simeq |V_{cb}|$ is well-known, ΔM_{B_d} essentially determines R_t, i.e. one side of the unitarity triangle. Even better, we can use the ratio $\Delta M_{B_d}/\Delta M_{B_s}$ for the same purpose: If one forms the ratio of the hadronic quantities in Eq. (103), many uncertainties drop out:

$$\xi \;=\; \frac{f_{B_s}\sqrt{\widehat{B}_{B_s}}}{f_{B_d}\sqrt{\widehat{B}_{B_d}}} \;=\; 1.20 \pm 0.06. \tag{111}$$

In the limit of exact flavour-SU(3) symmetry (corresponding to $m_u = m_d = m_s$) one has $\xi = 1$ which reduces the calculational task to compute the deviation of ξ from 1. The somewhat large error in Eq. (111) reflects the ongoing discussion on potentially large chiral logarithms [21] which may increase ξ significantly. This problem occurs, because lattice simulations use values for the pion mass which are larger than the physical value. The extrapolation to $m_\pi \simeq 140\,\text{MeV}$ with the help of chiral perturbation theory introduces this source of error. Sum-rule calculations of ξ (or rather f_{B_s}/f_{B_d}) which automatically include these logarithms, however, give values at the lower end of the range in Eq. (111) [22]. Further all short-distance QCD drops out from the ratio $\Delta M_{B_d}/\Delta M_{B_s}$, so that one simply has

$$\left| \frac{V_{td}}{V_{ts}} \right| \;=\; \sqrt{\frac{\Delta M_{B_d}}{\Delta M_{B_s}}} \sqrt{\frac{M_{B_s}}{M_{B_d}}}\, \xi. \tag{112}$$

The Wolfenstein expansion leads to

$$\left| \frac{V_{td}}{V_{ts}} \right| \;=\; R_t\lambda \left[1 + \lambda^2 \left(\frac{1}{2} - \overline{\rho} \right) + \mathcal{O}(\lambda^4) \right]. \tag{113}$$

Combining Eqs. (112) and (113) (and using $M_{B_s}/M_{B_d} = 1.017$) we easily derive a home-use formula for R_t:

$$R_t \;=\; 0.887\, \frac{\Delta M_{B_d}}{0.507\,\text{ps}^{-1}}\, \frac{17.77\,\text{ps}^{-1}}{\Delta M_{B_s}}\, \frac{\xi}{1.2}\, \frac{\lambda}{0.2246}\, [1 + 0.05\,\overline{\rho}\,] \tag{114}$$

Neither $\overline{\rho} \approx 0.2$ nor the 1% error on $\lambda \simeq 0.2246$ have an impact on the error of R_t. Using the numerical input from Eqs. (107–108) and Eq. (111) we find

$$R_t \;=\; 0.90 \pm 0.04 \tag{115}$$

and the uncertainty is essentially solely from ξ in Eq. (111).

Next we discuss $\Delta\Gamma$ and the quantity a_{fs} in Eq. (57), which governs *CP* violation in mixing. In order to find these quantities we need to calculate Γ_{12}. This involves the diagrams of Fig. 5 and brings in a new feature, power corrections of order Λ_{QCD}/m_b [23]. NLL QCD corrections to Γ_{12} in the B system have been calculated in Ref. [24–26]. In the SM the *CP* phase ϕ of Eq. (38) is so small that one can set $\cos\phi$ to 1 in Eq. (45). If we normalise $\Delta\Gamma$ to ΔM we can eliminate the bulk of the hadronic uncertainties. Updated values, obtained by using an improved operator basis, are [27]

$$\Delta\Gamma_{B_s} = \left(\frac{\Delta\Gamma_{B_s}}{\Delta M_{B_s}}\right)^{\text{th}} \Delta M_{B_s}^{\text{exp}} = 0.088 \pm 0.017\,\text{ps}^{-1}, \tag{116}$$

$$\Delta\Gamma_{B_d} = \left(\frac{\Delta\Gamma_{B_d}}{\Delta M_{B_d}}\right)^{\text{th}} \Delta M_{B_d}^{\text{exp}} = \left(26.7^{+5.8}_{-6.5}\right) \cdot 10^{-4}\,\text{ps}^{-1}. \tag{117}$$

The width difference in the B_s system amounts to $12.7 \pm 2.4\%$ of the average width $\Gamma_{B_s} \simeq \Gamma_{B_d}$ [27] and is in the reach of present experiments. Needless to say that there are no useful data on $\Delta\Gamma_{B_d}$. The predictions for the *CP* asymmetries in flavour-specific decays of Eq. (57) are calculated from Eq. (43) and read [25–27]

$$a_{\text{fs}}^s = (2.06 \pm 0.57) \cdot 10^{-5} \tag{118}$$

$$a_{\text{fs}}^d = \left(-4.8^{+1.0}_{-1.2}\right) \cdot 10^{-4}. \tag{119}$$

Also the current data for these *CP* asymmetries are not useful for CKM metrology. A future measurement of $a_{\text{fs}}^{d\,\text{exp}}$ will add an interesting new constraint to the $(\overline{\rho}, \overline{\eta})$ plane [25]:

$$(\overline{\eta} - R_{\text{fs}})^2 + (1-\overline{\rho})^2 = R_{\text{fs}}^2 \qquad \text{with} \qquad R_{\text{fs}} = -\frac{a_{\text{fs}}^{d\,\text{exp}}}{\left(10.1^{+1.8}_{-1.7}\right) \cdot 10^{-4}}. \tag{120}$$

The theory prediction of Refs. [25, 26] enters the denominator of R_{fs}, the quoted value is consistent with Eq. (119) and stems from the update in Ref. [27]. Eq. (120) defines a circle with radius R_{fs} centred around $(\overline{\rho}, \overline{\eta}) = (1, R_{\text{fs}})$. Therefore the circle touches the $\overline{\rho}$ axis at the point $(1, 0)$, see Fig. 6.

We have seen that the three quantities related to $B_s - \overline{B}_s$ mixing discussed in Eqs. (106), (116) and (118) have little dependence on $\overline{\rho}$ and $\overline{\eta}$. Only ΔM_{B_s} has an impact on CKM metrology, through Eq. (114). The small sensitivity to $\overline{\rho}$ and $\overline{\eta}$ becomes a virtue in searches for new physics, where $B_s - \overline{B}_s$ mixing plays an important role.

Next we discuss $K - \overline{K}$ mixing: The calculation of M_{12} now forces us to compute box diagrams of Fig. 1 with all possible quark flavours u, c, t, because the top contribution involving $S(x_t)$ is suppressed by the small CKM factor $(V_{ts}^* V_{td})^2 \simeq A^4\lambda^{10}(1 - \overline{\rho} + i\overline{\eta})^2$. The charm and up contributions, however, are proportional to only two powers of λ. Therefore we cannot neglect these contributions despite of the smallness of $S(x_c)$ and $S(x_c, x_t)$ (discussed around Eq. (91)). Their calculation proceeds in two major steps: First, the top quark and W-boson are integrated out. In the resulting effective theory the $\Delta S = 2$ transitions receive second-order contributions from a $|\Delta S| = 1$-Hamiltonian $H^{|\Delta S|=1}$. We have already seen this in our discussion of $\Delta B = 2$ transitions, the corresponding expression for $K - \overline{K}$ mixing is obtained by replacing $H^{|\Delta B|=1}$ with $H^{|\Delta S|=1}$ in Eq. (105) (and is described by the analogous diagrams of Fig. 5). In addition to this bilocal contribution, the term with $S(x_c, x_t)$ also involves a $|\Delta S| = 2$-Hamiltonian $H^{|\Delta S|=2}$ which mediates $K - \overline{K}$ mixing via a local

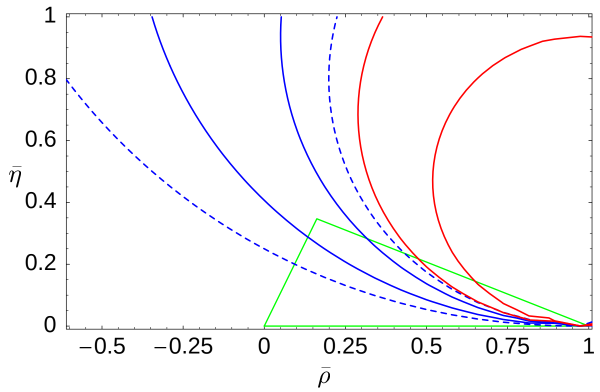

Figure 6: Impact of $a_{\rm fs}^d$ on the $(\overline{\rho}, \overline{\eta})$ plane: The solid blue curves limit the allowed range (defined by the error in Eq. (120)) for a hypothetical measurement of $a_{\rm fs}^{d\,\rm exp} = -5 \cdot 10^{-4}$. The solid red curves are for $a_{\rm fs}^{d\,\rm exp} = -10^{-3}$ instead. For further information see Ref. [25], from which the figure is taken.

four-quark operator, just as in the case of $B-\overline{B}$ mixing. The $|\Delta S| = 1$ and $|\Delta S| = 2$ Wilson coefficients of this effective field theory are evolved down to the scale $\mu_{bc} = \mathcal{O}(m_c)$ at which the second step of the calculation is performed: Now the bottom and charm quarks are integrated out and the effective field theory set up in the first step is matched to another effective field theory. The new theory treats m_b and m_c as heavy scales, so that all box diagrams involving at least one charm quark are effectively contracted to a point. All information on m_c (and m_b which plays a minor role) resides in the Wilson coefficient of the local $\Delta S = 2$ operator

$$Q = \overline{d}_L \gamma_\nu s_L \, \overline{d}_L \gamma^\nu s_L . \qquad (121)$$

The effective $|\Delta S| = 2$ Hamiltonian can therefore be written in a similar way as the $|\Delta B| = 2$ Hamiltonian of Eq. (101):

$$H^{|\Delta S|=2} = \frac{G_F^2}{4\pi^2} M_W^2 \, \left[(V_{ts} V_{td}^*)^2 \, \eta_{tt} \, S(x_t) \, + \, 2 V_{ts} V_{td}^* V_{cs} V_{cd}^* \, \eta_{ct} \, S(x_c, x_t) \right. \\ \left. + \, (V_{cs} V_{cd}^*)^2 \, \eta_{cc} \, x_c \right] \, b_K(\mu_K) Q(\mu_K) \, + \, h.c. \qquad (122)$$

The NLL results for the short-distance QCD factors read

$$\eta_{tt} = 0.57, \qquad \eta_{ct} = 0.47 \pm 0.05, \qquad \eta_{cc} = (1.44 \pm 0.35) \left(\frac{1.3\,\text{GeV}}{m_c} \right)^{1.1} . \qquad (123)$$

The QCD coefficients in Eq. (123) were calculated to LL accuracy in Ref. [30]. The NLL calculation of η_{tt} [18] is analogous to that of η_B, with one new feature: When crossing the threshold μ_{bc} one must change the number of active flavours in the QCD β function and the NLL anomalous dimension γ_+ from $f = 5$ to $f = 3$. The NLL results for η_{ct} [31] and η_{cc} [32] have a sizable uncertainty, because they are sensitive to the low scale of $\mu_{bc} \sim m_c$ where α_s is large. η_{cc} also exhibits a sizable dependence on $\alpha_s(M_Z)$ and on $m_c = m_c(m_c)$, so that the central values quoted in the literature vary over some range. The expression in Eq. (123) approximates the dependence on m_c and corresponds to $\alpha_s(M_Z) = 0.119 \pm 0.002$. The scale μ_K must be chosen below m_c and is typically taken around 1 GeV, where perturbation theory is still applicable. One finds $b_K(\mu_K = 1\,\text{GeV}) = 1.24 \pm 0.02$ and the error stems from the uncertainty in α_s.

In the discussion of $|\Delta S| = 2$ transitions we must also address corrections of order $m_{\mathrm{light}}^2/m_{\mathrm{heavy}}^2$ which correspond to subleading terms in the operator product expansion of Eq. (79). While these corrections are of order $\Lambda_{\mathrm{QCD}}^2/m_t^2$ for the first term in $H^{|\Delta S|=2}$, they are of order $\Lambda_{\mathrm{QCD}}^2/m_c^2$ in the case of the charm contributions involving $S(x_c, x_t) = \mathcal{O}(x_c \ln x_c)$ and $S(x_c) \simeq x_c$ in Eq. (122). The largest of these power corrections involves two $|\Delta S| = 1$ operators and corresponds to the box diagram in Fig. 1 with two internal up-quarks. To understand the power counting, recall that the charm contribution in $H^{|\Delta S|=2}$ is proportional to $M_W^2 x_c = m_c^2$, while the box with up-quarks involves no power of m_c, so that its size is characterised by the hadronic energy scale Λ_{QCD}. Including this bilocal contribution we write:

$$M_{12} = \frac{1}{2m_K} \langle K|H^{|\Delta S|=2}|\overline{K}\rangle - \text{Disp}\, \frac{i}{4m_K} \int d^4x \, \langle K|H^{|\Delta S|=1}(x)\, H^{|\Delta S|=1}(0)|\overline{K}\rangle \, . \qquad (124)$$

Here "Disp" denotes the dispersive part of the matrix element, which is introduced in Eq. (24) and is discussed after Eq. (104). The enhancement of the second term stems from the so-called $\Delta I = 0$ *rule* which describes the non-perturbative enhancement of the decay $K_{\mathrm{short}} \to (\pi\pi)_{I=0}$. The two terms in Eq. (124) are usually referred to as *short-distance* and *long-distance* contributions. The long-distance contribution has defied any reliable calculation from first principles so far. In this humbling situation we can only compare the experimental value of ΔM_K to the short-distance contribution

$$\Delta M_K^{\mathrm{SD}} = \frac{|\langle K|H^{|\Delta S|=2}|\overline{K}\rangle|}{m_K} \, . \qquad (125)$$

In order to compute ΔM_K^{SD} we need the hadronic matrix element

$$\langle K|Q(\mu_K)|\overline{K}\rangle \;\; = \;\; \frac{2}{3} M_K^2 \, f_K^2 \, \frac{\widehat{B}_K}{b_K(\mu_K)} . \qquad (126)$$

Contrary to the situation in the B system, the Kaon decay constant $f_K = 160\,\mathrm{MeV}$ is well-measured. We remark here that we know $\widehat{B}_K$ in a particular limit of QCD: If the number of colours N_c is taken to infinity, $\langle K|Q(\mu_K)|\overline{K}\rangle$ can be expressed in terms of the current matrix element $\langle 0|\overline{d}_L \gamma_\nu s_L|\overline{K}\rangle$ which defines f_K. For $N_c = \infty$ one finds $\widehat{B}_K/b_K(\mu_K) = 3/4$; including certain calculable ("factorisable") $1/N_c$ corrections changes this to $\widehat{B}_K/b_K(\mu_K) = 1$. A recent lattice calculation finds [33]

$$\widehat{B}_K \;\; = \;\; 0.72 \pm 0.04. \qquad (127)$$

The experimental value of the K_{long}–K_{short} mass difference is [8]

$$\Delta M_K^{\mathrm{exp}} \;\; = \;\; (3.483 \pm 0.006)\;\mu\mathrm{eV} \;\; = \;\; (5.292 \pm 0.009) \cdot 10^{-3}\,\mathrm{ps}^{-1}. \qquad (128)$$

Inserting Eqs. (122) and (126) into Eq. (125) gives

$$\frac{\Delta M_K^{\mathrm{SD}}}{\Delta M_K^{\mathrm{exp}}} \;\; = \;\; (0.98 \pm 0.22) \widehat{B}_K. \qquad (129)$$

ΔM_K^{SD} is dominated by the term proportional to $(V_{cs}V_{cd}^*)^2$ and the error in Eq. (129) essentially stems from η_{cc} in Eq. (123). This uncertainty will shrink when η_{cc} is calculated to NNLL accuracy. With Eq. (127) we find that $H^{|\Delta S|=2}$ contributes $(70 \pm 25)\%$ to the measured ΔM_K.

The off-diagonal element of the decay matrix is given by

$$\Gamma_{12} \;=\; \text{Abs}\, \frac{i}{2m_K} \int d^4x \,\langle K|H^{|\Delta S|=1}(x)\, H^{|\Delta S|=1}(0)|\overline{K}\rangle \tag{130}$$

$$= \frac{1}{2m_K} \sum_f (2\pi)^4 \delta^4(p_K - p_f) \langle K|H^{|\Delta S|=1}|f\rangle \,\langle f|H^{|\Delta S|=1}|\overline{K}\rangle \simeq \frac{1}{2m_K}\, A_0^* \,\overline{A}_0\,. \tag{131}$$

Here "Abs" denotes the absorptive part of the matrix element. Γ_{12} is an inclusive quantity built out of all final states f into which both K and $\overline{K}$ can decay. A special feature of the neutral Kaon system is the saturation of Γ_{12} by a single decay mode, which is $K \to (\pi\pi)_{I=0}$. The notation A_0 and $\overline{A}_0$ for the corresponding decay amplitudes has been introduced after Eq. (14). Γ_{12} is a non-perturbative quantity and its computation on the lattice involves the difficult task to understand and master the $\Delta I = 0$ rule. The relation between Γ_{12} and $\Delta\Gamma_K$ has been derived in Eq. (45). Experimentally we have [8]

$$\Delta\Gamma_K^{\rm exp} \;=\; (7.335 \pm 0.004)\,\mu\text{eV} \;=\; (11.144 \pm 0.006) \cdot 10^{-3}\,\text{ps}^{-1}. \tag{132}$$

With Eqs. (128) and (132) we have precise experimental information on $|M_{12}| \simeq \Delta M_K/2$ and $|\Gamma_{12}| \simeq \Delta\Gamma_K/2$. To fully characterise $K-\overline{K}$ mixing we also need to know the phase ϕ defined in Eq. (38). As in the case of $B-\overline{B}$ mixing we study a *CP* asymmetry in a flavour-specific decay mode. With Eqs. (11) and (41) one easily finds

$$A_L \;\equiv\; \frac{\Gamma(K_{\rm long} \to \ell^+\nu\,\pi^-) - \Gamma(K_{\rm long} \to \ell^-\overline{\nu}\,\pi^+)}{\Gamma(K_{\rm long} \to \ell^+\nu\,\pi^-) + \Gamma(K_{\rm long} \to \ell^-\overline{\nu}\,\pi^+)}$$

$$= \frac{1-|q/p|^2}{1+|q/p|^2} \;\simeq\; \frac{a}{2}. \tag{133}$$

At this point it is worthwhile to look back at the quantity ϵ_K which we have encountered in the first lecture in Eq. (14). From Eq. (17) we have learned that $\text{Re}\,\epsilon_K$ measures CP violation in mixing quantified by $1-|q/p|$, just as A_L in Eq. (133). While $\text{Im}\,\epsilon_K$ is related to a different physical phenomenon, namely mixing-induced *CP* violation, it provides the very same information on the fundamental parameters of $K-\overline{K}$ mixing: Since $K \to (\pi\pi)_{I=0}$ dominates Γ_{12}, the *CP*-violating phase of $\overline{A}_0/A_0$ equals $\arg\Gamma_{12}$, see Eq. (131). With this observation and the help of Eq. (42) we can express ϵ_K in Eq. (17) entirely in terms of ΔM_K, $\Delta\Gamma_K$ and ϕ. Interestingly, the phase ϕ_ϵ of ϵ_K (see Eq. (14)) is simply given by

$$\phi_\epsilon \;=\; \arctan\frac{\Delta M_K}{\Delta\Gamma_K/2}. \tag{134}$$

More details of this calculation can be found in Chapter 1.6 of Ref. [34]. Nature chose $\Delta M_K \approx \Delta\Gamma_K/2$ by accident, so that ϕ_ϵ in Eq. (14) is close to 45°. The bottom line is that ϕ_ϵ carries no information on *CP* violation and that $|\epsilon_K|$ and A_L involve the same fundamental *CP*-violating quantity, which is ϕ. To extract ϕ from A_L in Eq. (133) or from ϵ_K in Eq. (17) we use Eq. (42), with $2|M_{12}|/|\Gamma_{12}| \simeq \Delta M_K/(\Delta\Gamma_K/2)$ traded for $\tan\phi_\epsilon$:

$$\begin{aligned} A_L &= \frac{1}{2}\sin(2\phi_\epsilon)\phi + \mathcal{O}(\phi^2) \\ \epsilon_K &\simeq \frac{1}{2}\sin(\phi_\epsilon)e^{i\phi_\epsilon}\phi + \mathcal{O}(\phi^2) \end{aligned} \tag{135}$$

Using the experimental value

$$A_L^{\rm exp} \;=\; (3.32 \pm 0.06) \times 10^{-3}$$

gives

$$\phi \;=\; (6.77 \pm 0.12) \times 10^{-3}. \tag{136}$$

This number is in reasonable agreement with $\phi = (6.48 \pm 0.03) \times 10^{-3}$ found from ϵ_K with Eq. (135). Next we relate ϕ to a constraint on $(\overline{\rho}, \overline{\eta})$: Specifying to the standard phase convention for the CKM matrix (with $V_{us}V_{ud}^*$ real and positive) we start from Eq. (38) to write

$$\phi \;=\; \arg\left(-\frac{M_{12}}{\Gamma_{12}}\right) \;\simeq\; \frac{\mathrm{Im}\, M_{12}}{|M_{12}|} - \arg(-\Gamma_{12}) \;=\; 2\left[\frac{\mathrm{Im}\, M_{12}}{\Delta M_K^{\mathrm{exp}}} + \xi_K\right] \tag{137}$$

where

$$2\xi_K \;\equiv\; -\arg(-\Gamma_{12}) \;\simeq\; -\arg\left(-\frac{\overline{A}_0}{A_0}\right). \tag{138}$$

In Eq. (137) I have used that the phases of M_{12} and $-\Gamma_{12}$ are separately small in the adopted phase convention and further traded $|M_{12}|$ for the experimental $\Delta M_K/2$. In Eq. (138) the saturation of Γ_{12} by $A_0^* \overline{A}_0$ in Eq. (131) has been used. Thus $-\xi_K$ is just the CP-odd phase in the decay $\overline{K} \to (\pi\pi)_{I=0}$. A recent analysis has estimated $\xi_K \approx -1.7 \cdot 10^{-4}$ [35], so that ξ_K contributes roughly -6% to the measured value of ϕ. The dominant term proportional to $\mathrm{Im}\, M_{12} = \mathrm{Im}\, \langle K|H^{|\Delta S|=2}|\overline{K}\rangle$ involves the CKM factors

$$\begin{aligned} \mathrm{Im}\,(V_{ts}V_{td}^*)^2 &\;\simeq\; 2(A\lambda^2)^4\lambda^2\,\overline{\eta}\,(1-\overline{\rho}) \\ \mathrm{Im}\,(2V_{ts}V_{td}^*V_{cs}V_{cd}^*) &\;\simeq\; -\mathrm{Im}\,(V_{cs}V_{cd}^*)^2 \simeq 2(A\lambda^2)^2\lambda^2\,\overline{\eta}, \end{aligned} \tag{139}$$

where the lowest-order Wolfenstein expansion has been used. Inspecting the dependences of the CKM factors on $\overline{\rho}$ and $\overline{\eta}$ we see that the experimental constraint from ϕ defines a hyperbola in the $(\overline{\rho}, \overline{\eta})$ plane. Combining Eq. (139) with Eqs. (122) and (137), inserting the QCD factors from Eq. (123) and the matrix element from Eq. (126) and finally using $\phi = (6.48 \pm 0.03) \times 10^{-3}$ from ϵ_K this hyperbola reads

$$\overline{\eta} \;=\; \frac{1}{\widehat{B}_K}\,\frac{0.34 \pm 0.03}{1.3 \pm 0.1 - \overline{\rho}}. \tag{140}$$

The uncertainties in $\widehat{B}_K$ from Eq. (127) and from η_{cc} and η_{ct} in Eq. (123) (reflected by 1.3 ± 0.1) inflict errors of similar size on the $\overline{\eta}$ extracted from Eq. (140). The numerator 0.34 ± 0.03 is calculated with $|V_{cb}| = A\lambda^2 = 0.0412 \pm 0.0011$. The 10% uncertainty of this number stems solely from the error in $|V_{cb}|$, which enters $\overline{\eta}$ in Eq. (140) with the fourth power.

The neutral Kaon system is the only neutral meson system for which all three quantities ΔM, $\Delta\Gamma$ and ϕ are measured. It should be stressed that also the sign of $\Delta\Gamma/\Delta M$ is firmly established. Measuring sign $(\Delta\Gamma/\Delta M)$ is difficult for all meson-antimeson systems. In the neutral Kaon system the measurement of ΔM and sign $(\Delta\Gamma/\Delta M)$ uses K_{short} *regeneration*: If a K_{long} beam hits a nucleus in a target (the regenerator), strong inelastic scattering changes the $|K_{\mathrm{long}}\rangle$ state into a superposition of $|K_{\mathrm{long}}\rangle$ and $|K_{\mathrm{short}}\rangle$ giving access to observables which are sensitive to ΔM and the abovementioned sign. For details on these experimental aspects I refer to [36].

Finally I discuss $D - \overline{D}$ mixing: Box diagrams in Fig. 1 with one or two internal b quarks are highly CKM-suppressed. The dominant box diagrams with internal d and s quarks suffer from a very efficient

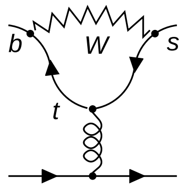

Figure 7: Gluonic penguin diagram with an internal top quark.

GIM suppression proportional to m_s^4/m_c^2. This makes the diagrams sensitive to very low scales and perturbative calculations of ΔM_D, $\Delta\Gamma_D$ and $a_{\rm fs}^D$ are put into doubt. In the effective theory both M_{12} and Γ_{12} are dominated by the bilocal contribution with $H^{|\Delta C|=1}$. The only possible clear prediction is the qualitative statement that all these quantities are very small. Theoretical calculations usually quote numbers for the quantities $x \equiv \Delta M_D/\Gamma_D$ and $y \equiv \Delta\Gamma_D/(2\Gamma_D)$. The theoretical predictions for $|x|, |y|$ cover the range from zero to $|x|, |y| \sim 0.01$ and come without reliable error estimates. Therefore current experimental values are compatible with the SM but may also be dominated by a new physics contribution. A "smoking gun" of new physics, however, would be the discovery of a non-zero CP asymmetry in the D system.

3.4 Mixing-induced *CP* asymmetries

At the end of Sect. 2.3 we have learned that mixing-induced *CP* asymmetries can provide clean information on fundamental *CP* phases in the Lagrangian. These *CP* asymmetries involve the interference between mixing and decay amplitudes as depicted on the right.

$$\begin{array}{ccc} B & \xrightarrow{q/p} & \overline{B} \\ A_f \searrow & & \swarrow \overline{A}_f \\ & f & \end{array}$$

In this lecture we restrict the discussion to gold-plated modes which involve a *CP* eigenstate $f_{\rm CP}$ in the final state, cf. Eq. (10).[5] In the B_d and B_s meson systems the mixing-induced *CP* asymmetries are a real gold mine, because there are many decay modes satisfying the condition for a golden decay mode as defined after Eq. (62). Prominent examples are the decays $B_s \to J/\psi\phi$ and $B_d \to J/\psi K_{\rm short}$, whose decay amplitudes essentially only involve the CKM factor $V_{cs}V_{cb}^*$. To understand this first note that the decay proceeds at tree–level by exchanging a W boson. There are also contributions involving an up, charm or top quark loop, with attached gluons splitting into the charm-anticharm pair hadronising into the J/ψ meson. Such diagrams are called *penguin diagrams*. A penguin diagram in the narrow sense only involves one neutral vector boson (which can be a gluon, photon or Z boson). A gluonic penguin diagram is depicted in Fig. 7. (Yet a J/ψ cannot be produced from a single gluon. One needs a photon or three gluons at least.) In the context of mixing-induced *CP* asymmetries one often speaks of *penguin pollution*, because the penguin diagrams may involve different CKM factors than the tree diagram spoiling the golden-mode property. To estimate the penguin pollution in $B_s \to J/\psi\phi$ and $B_d \to J/\psi K_{\rm short}$ first use the unitarity relation $V_{ts}V_{tb}^* = -V_{cs}V_{cb}^* - V_{us}V_{ub}^*$ to write

$$H^{|\Delta B|=1} \quad = \quad V_{cs}V_{cb}^* h_c + V_{cs}^* V_{cb} h_c^\dagger + V_{us}V_{ub}^* h_u + V_{us}^* V_{ub} h_u^\dagger . \qquad (141)$$

Here the last two terms are highly suppressed, since $|V_{us}^* V_{ub}| \sim 0.03\,|V_{cs}^* V_{cb}|$. Moreover, h_u has no tree contributions, but solely stems from penguin diagrams with up and top quarks. Since these loop

[5]One can also identify gold-plated decays into non-CP eigenstates, important channels are e.g. $B_s \to D_s^\pm K^\mp$.

effects involve non-perturbative physics, it is difficult to quantify the loop suppression. Still, the CKM suppression is efficient enough to render the modes gold-plated at the level of a few percent. Since the CKM elements are factored out in Eq. (141), h_c and h_u only contain Wilson coefficients, operators and real constants. Importantly, $h_{u,c}$ and $h_{u,c}^\dagger$ are related by the *CP* transformation:

$$h_{u,c}^\dagger \quad = \quad (CP)^\dagger h_{u,c} CP. \tag{142}$$

While I discuss $B_s \to J/\psi\phi$ and $B_d \to J/\psi K_{\text{short}}$ here for definiteness, the results apply to other gold-plated $M \to f_{\text{CP}}$ modes as well, with obvious replacements for the CKM elements. The underlying reason for the cancellation of hadronic uncertainties in gold-plated decays is the *CP* invariance of QCD: While we cannot compute $\langle f_{\text{CP}}|h_c|B\rangle$[6], we can relate this matrix element to $\langle f_{\text{CP}}|h_c^\dagger|\overline{B}\rangle$ through

$$\langle f_{\text{CP}}|h_{u,c}^\dagger|\overline{B}\rangle \quad = \quad \langle f_{\text{CP}}|(CP)^\dagger h_{u,c} CP|\overline{B}\rangle \;=\; -\eta_{\text{CP}}\langle f_{\text{CP}}|h_{u,c}|B\rangle, \tag{143}$$

where I just used the *CP* transformations of Eqs. (9–10) and Eq. (142). We first apply this to the decay mode $B_s \to J/\psi\phi$. The final state consists of two vector mesons. By conservation of angular momentum they can be in states with orbital angular momentum quantum numbers $l = 0, 1$ or 2: The two spin-1 states of the vector mesons can be added to a state of total spin $0, 1$ or 2, which requires an orbital angular momentum of $l = 0, 1$ or 2 to give a $J/\psi\phi$ state with zero total angular momentum. The p-wave state with $l = 1$ is *CP*-odd and the other two states are *CP*-even, owing to the parity quantum number $(-1)^l$ of their spatial wave function. Experimentally one separates these states by an angular analysis [37, 38] of the data sample. This can be done including the full time dependence of the decay, so that we can isolate the time-dependent *CP* asymmetries in the different partial-wave channels. The most-populated state is the CP-even $l = 0$ (i.e. s-wave) state. Writing $f_{\text{CP}} = (J/\psi\phi)_l$ with $\eta_{\text{CP}} = (-1)^l$ we obtain for the amplitudes $A_{f_{\text{CP}}}$ and $\overline{A}_{f_{\text{CP}}}$ (see Eq. (12)):

$$\frac{\overline{A}_{f_{\text{CP}}}}{A_{f_{\text{CP}}}} \quad \simeq \quad \frac{\langle f_{\text{CP}}|H^{|\Delta B|=1}|\overline{B}_s\rangle}{\langle f_{\text{CP}}|H^{|\Delta B|=1}|B_s\rangle} \;=\; \frac{V_{cs}^* V_{cb}}{V_{cs} V_{cb}^*}\frac{\langle f_{\text{CP}}|h_c^\dagger|\overline{B}_s\rangle}{\langle f_{\text{CP}}|h_c|B_s\rangle} \;=\; -\eta_{\text{CP}}\frac{V_{cs}^* V_{cb}}{V_{cs} V_{cb}^*} \tag{144}$$

Combining this result with Eqs. (47) and (13) we find

$$\lambda_{f_{\text{CP}}} \quad = \quad \eta_{\text{CP}} \frac{V_{tb}^* V_{ts}}{V_{tb} V_{ts}^*}\frac{V_{cs}^* V_{cb}}{V_{cs} V_{cb}^*} \;=\; \eta_{\text{CP}}\, e^{2i\beta_s}. \tag{145}$$

In the last step I have used the definition of β_s in Eq. (77). With Eq. (145) we can calculate the time-dependent *CP* asymmetry of Eq. (61). First we verify that our golden mode satisfies $|\lambda_{f_{\text{CP}}}| = 1$, so that A_{CP}^{dir} in Eq. (62) vanishes. The other two quantities in Eq. (61) evaluate with Eq. (145) to $A_{CP}^{\text{mix}} = -\eta_{\text{CP}} \sin(2\beta_s)$ and $A_{\Delta\Gamma} = -\eta_{\text{CP}}\cos(2\beta_s)$, so that (neglecting the tiny $\mathcal{O}(a)$ term)

$$a_{f_{\text{CP}}}(t) = \eta_{\text{CP}} \frac{\sin(2\beta_s)\sin(\Delta M_{B_s} t)}{\cosh(\Delta\Gamma_{B_s} t/2) - \eta_{\text{CP}}\cos(2\beta_s)\sinh(\Delta\Gamma_{B_s} t/2)} \qquad \text{for } f_{\text{CP}} = (J/\psi\phi)_l. \tag{146}$$

In the SM β_s is small and $a_{(J/\psi\phi)_l}(t)$ is an ideal testing ground to find new physics [27, 38].

Next I discuss $B_d \to J/\psi K_{\text{short}}$. The final state has orbital angular momentum $l = 1$ balancing the spin of the J/ψ. Neglecting the small *CP* violation in $K-\overline{K}$ mixing we can regard the K_{short}

[6] In flavour physics matrix elements like $\langle f|H^{|\Delta B|=1}|M\rangle$ are always understood to include the strong interaction. This means that the fields are understood as interacting fields in the Heisenberg picture with respect to the strong interaction.

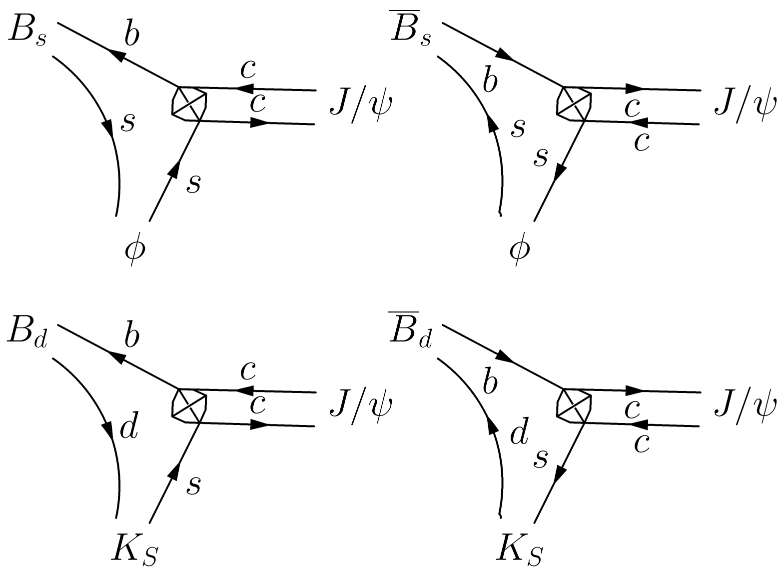

Figure 8: Interfering amplitudes which give rise to mixing-induced CP violation for the two golden modes discussed in the text.

as *CP*-even. The J/ψ is *CP*-even as well and the orbital angular momentum contributes a factor of -1 to the total *CP* quantum number. Thus $\eta_{J/\psi K_{\rm short}} = -1$. From Fig. 8 we observe a novel feature compared to $B_s \to J/\psi\phi$. The interference of the B_d and $\overline{B}_d$ decays involves $K-\overline{K}$ mixing: The B_d decay involves the K component of $K_{\rm short}$, while the $\overline{B}_d$ decays into the $\overline{K}$ component of $K_{\rm short}$. Experimentally the $K_{\rm short}$ is detected via a pair of charged pions whose invariant mass equals M_K, denoted here by $(\pi^+\pi^-)_K$. Therefore we should identify the amplitudes $A_{f_{\rm CP}=J/\psi K_{\rm short}}$ and $\overline{A}_{f_{\rm CP}=J/\psi K_{\rm short}}$ with $A(B_d \to J/\psi K \to J/\psi(\pi^+\pi^-)_K)$ and $\overline{A}(\overline{B}_d \to J/\psi \overline{K} \to J/\psi(\pi^+\pi^-)_K)$, respectively. Therefore

$$\frac{\overline{A}_{J/\psi K_{\rm short}}}{A_{J/\psi K_{\rm short}}} = \frac{V_{cb}V_{cs}^*}{V_{cb}^*V_{cs}}\frac{V_{us}V_{ud}^*}{V_{us}^*V_{ud}}, \qquad \lambda_{J/\psi K_{\rm short}} = -\frac{V_{tb}^*V_{td}}{V_{tb}V_{td}^*}\frac{V_{cb}V_{cs}^*}{V_{cb}^*V_{cs}}\frac{V_{us}V_{ud}^*}{V_{us}^*V_{ud}} \simeq -e^{-2i\beta} \tag{147}$$

In the last step I have used the definition of β in Eq. (72) and neglected $\arg[-V_{cd}V_{cs}^*/(V_{ud}V_{us}^*)] \simeq A^2\lambda^4\overline{\eta} < 10^{-3}$, so that $\mathrm{Im}\,\lambda_{J/\psi K_{\rm short}} \simeq \sin(2\beta)$. We may further neglect $\Delta\Gamma_{B_d}$ in Eq. (61) to find the most famous time-dependent *CP* asymmetry,

$$a_{J/\psi K_{\rm short}}(t) = \sin(2\beta)\sin(\Delta M_{B_d} t). \tag{148}$$

Finally I give a (very incomplete) list of other golden $M \to f_{\rm CP}$ decays. The decay $B_s \to J/\psi\phi$ can be substituted for $B_s \to J/\psi\eta^{(\prime)}$, which does not require any angular decomposition. In a hadron collider experiment η's and η''s are hard to detect, but $B_s \to J/\psi\eta^{(\prime)}$ is interesting for B factories running on the $\Upsilon(5S)$ resonance. While the modes discussed above provide insight into the physics of B–$\overline{B}$ mixing, one can also use mixing-induced *CP* violation to probe *CP* phases from new physics in loop-induced B decays such as $B_d \to \phi K_{\rm short}$ [39]. This mode is triggered by the quark decay $\overline{b} \to \overline{s}s\overline{s}$. The same transition in probed in $B_s \to \phi\phi$. Likewise new physics in the $\overline{b} \to \overline{s}d\overline{d}$ amplitude may reveal itself in $B_s \to K_{\rm short}K_{\rm short}$. Gold-plated D^0 decays are $D^0 \to K_{\rm short}\pi^0$ and $D^0 \to K_{\rm short}\rho^0$, which are penguin-free $c \to s\overline{d}u$ decays. A gold-plated K decay is $K_{\text{long}} \to \pi^0 \nu\overline{\nu}$ [40]. Here no meson-antimeson oscillations are present, but $K-\overline{K}$ mixing nevertheless enters the process through the mass eigenstate K_{long}. The final state $\pi^0\nu\overline{\nu}$ is *CP*-even and the dominant contribution to the decay involves mixing-induced *CP* violation, i.e. the decay amplitude is proportional to $\operatorname{Im}\lambda_f$ (see e.g. Ref [41]).

3.5 The unitarity triangle

Many measurements contribute to the global fit of the unitarity triangle defined in Eq. (70) and depicted in Fig. 3. Conceptually it is useful to disentangle tree decays from FCNC processes: Tree-level amplitudes are insensitive to new physics and therefore determine the true apex $(\overline{\rho}, \overline{\eta})$ of the unitarity triangle. In principle one could determine the unitarity triangle in this way, insert the result into the SM predictions of the FCNC processes and then assess the possible impact of new physics on the latter. In practice, however, the tree constraints still suffer from large uncertainties, while for example $a_{J/\psi K_{\text{short}}}(t)$ in Eq. (148) and $\Delta M_{B_d}/\Delta M_{B_s}$ in Eq. (114) determine $\sin(2\beta)$ and the side R_t (see Eq. (71)) fairly precisely. Therefore, for the time being, it is best to combine all information into a global fit of the unitarity triangle.

From $b \to c\ell\overline{\nu}$ decays $|V_{cb}| \simeq A\lambda^2$ is precisely determined. Therefore we realise from Eqs. (71) and (76) that any measurement of $|V_{ub}|$ essentially fixes the side R_u of the triangle. $|V_{ub}|$ is determined from (inclusive or exclusive) semileptonic $b \to u$ decays and hadronic uncertainties limit the accuracy of the extracted $|V_{ub}|$ to 8-10%. The theoretical methods used to determine $|V_{cb}|$ and $|V_{ub}|$ are briefly reviewed in Ref. [42]. The angle γ of the unitarity triangle is currently measured in two ways from tree-level decays: First, the interference of the $b \to c\overline{u}s$ and $b \to u\overline{c}s$ amplitudes in $B^\pm \to \overset{(-)}{D} K^\pm$ decays is exploited [43]. Second, one measures mixing-induced *CP* violation in $B_d \to \pi\pi$, $B_d \to \rho\pi$ or $B_d \to \rho\rho$ decays, which allows to find the angle α of the desired triangle. These modes are not gold-plated and suffer from penguin pollution, which, however, can be eliminated by means of an isospin analysis [44]. While the extracted result for α is sensitive to new physics in $B_d-\overline{B}_d$ mixing, this possible effect can be eliminated if the measured α^{exp} and β^{exp} are combined to give $\gamma^{\text{exp}} = \pi - \alpha^{\text{exp}} - \beta^{\text{exp}}$. Combining the constraints from $|V_{ub}|$, γ and α with those from meson-antimeson mixing discussed in this lecture results in the unitarity triangle shown in Fig. 9.

Suggestions for further reading

There are many good review articles on meson-antimeson mixing and flavour physics in general, putting emphasis on different aspects of the field. A student interested in the theoretical foundation of flavour physics, effective Hamiltonians and higher-order calculations is referred to the lecture in Ref. [48] and the review articles in Refs. [34, 49]. Most reviews and lectures focus on CP violation and I recommend Refs. [47] and [50]. I have only briefly touched $D-\overline{D}$ mixing, two review articles dedicated to D physics are cited in Ref. [51]. Lectures covering both K and D physics can be found in Ref. [52]. A concise summary of the physics entering CKM metrology can be found in Ref. [42], a more elaborate article on the subject is Ref. [53]. Standard textbooks on flavour physics are listed in Ref. [54].

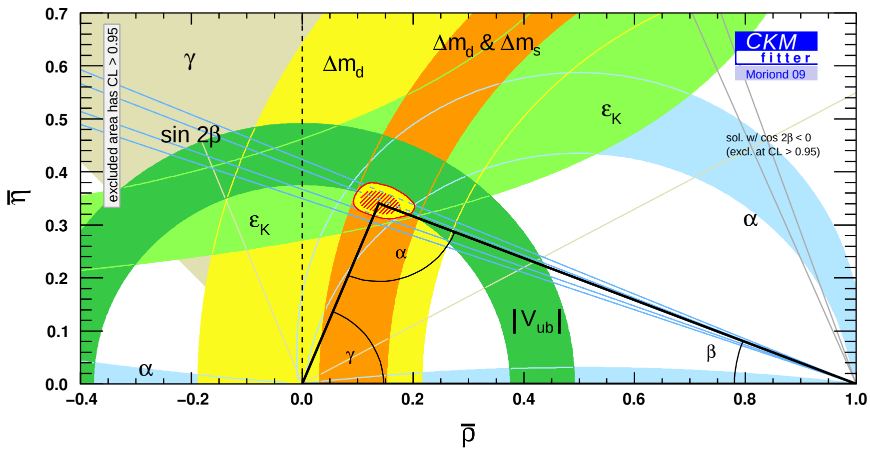

Figure 9: Global fit to the unitarity triangle from the CKMFitter group [45]. A different statistical approach is used by the UTFit group [46].

Acknowledgements

I am grateful to Ahmed Ali and Misha Ivanov for the invitation to this summer school. It has been a pleasure to discuss so many different fields of physics with the other lecturers and the participating students. I thank Momchil Davidkov, Lars Hofer and Dominik Scherer for proofreading this text.

References

[1] D. J. Gross and F. Wilczek, Phys. Rev. Lett., **30** (1973) 1343.
H. D. Politzer, Phys. Rev. **30** (1973) 1346.

[2] S. L. Glashow, J. Iliopoulos and L. Maiani, Phys. Rev. **D2** (1970) 1285.

[3] M. K. Gaillard and B. W. Lee, Phys. Rev. **D10** (1974) 897.

[4] J. H. Christenson, J. W. Cronin, V. L. Fitch and R. Turlay, Phys. Rev. Lett. **13** (1964) 138; Phys. Rev. **140B** (1965) 74.

[5] S. L. Glashow, Nucl. Phys. **22** (1961) 579. S. Weinberg, Phys. Rev. Lett. **19** (1967) 1264. A. Salam in *Elementary Particle Physics (Nobel Symp. 8)*, ed. N. Svartholm, Almquist and Wilsell, Stockholm, 1968.

[6] M. Kobayashi and T. Maskawa, Progr. Theor. Phys. **49** (1973) 652.

[7] H. Albrecht *et al.* [ARGUS Collaboration], Phys. Lett. B **192** (1987) 245.

[8] C. Amsler *et al.* [Particle Data Group], Phys. Lett. B **667** (2008) 1.

[9] G. Lüders, Dan. Mat. Phys. Medd. **28** (1954) 5; W. Pauli in *Niels Bohr and the Development of Physics*, ed. W. Pauli, L. Rosenfeld and V. Weisskopf (McGraw-Hill, New York, 1955); G. Lüders, Ann. Phys. **2** (1957).

[10] L.A. Khalfin, Zh. Eksp. Teor. Fiz. **33** (1957) 1371.

[11] V.F. Weisskopf and E.P. Wigner, Z. Phys. **63** (1930) 54; **65** (1930) 18; T. D. Lee, R. Oehme and C. N. Yang, Phys. Rev. **106** (1957) 340.

[12] P. K. Kabir, *The CP puzzle: strange decays of the neutral Kaon*, Acad. Pr., London, 1968. O. Nachtmann, *Elementary particle physics : concepts and phenomena*, Springer, Berlin, 1990.

[13] C. B. Chiu and E. C. G. Sudarshan, Phys. Rev. D **42** (1990) 3712.

[14] A. Abulencia *et al.* [CDF Collaboration], Phys. Rev. Lett. **97** (2006) 242003 [arXiv:hep-ex/0609040].

[15] L. Wolfenstein, Phys. Rev. Lett. **51** (1983) 1945.

[16] C. Jarlskog, Phys. Rev. Lett. **55** (1985) 1039.

[17] A. J. Buras, M. E. Lautenbacher, G. Ostermaier, Phys. Rev. D **50** (1994) 3433.

[18] A. J. Buras, M. Jamin and P. H. Weisz, Nucl. Phys. B **347** (1990) 491.

[19] A. J. Buras and P. H. Weisz, Nucl. Phys. B **333** (1990) 66.

[20] V. M. Abazov *et al.* [DØ Collaboration], Phys. Rev. Lett. **97** (2006) 021802 [arXiv:hep-ex/0603029]; DØ Note 5618-CONF.

[21] A. S. Kronfeld and S. M. Ryan, Phys. Lett. B **543** (2002) 59 [arXiv:hep-ph/0206058]. D. Becirevic, S. Fajfer, S. Prelovsek and J. Zupan, Phys. Lett. B **563** (2003) 150 [arXiv:hep-ph/0211271]. V. Gadiyak and O. Loktik, Phys. Rev. D **72** (2005) 114504 [arXiv:hep-lat/0509075]. D. Becirevic, S. Fajfer and J. F. Kamenik, JHEP **0706** (2007) 003 [arXiv:hep-ph/0612224].

[22] M. Jamin and B. O. Lange, Phys. Rev. D **65** (2002) 056005 [arXiv:hep-ph/0108135].

[23] M. Beneke, G. Buchalla and I. Dunietz, Phys. Rev. **D54**, 4419 (1996). A. S. Dighe, T. Hurth, C. S. Kim and T. Yoshikawa, Nucl. Phys. B **624** (2002) 377 [arXiv:hep-ph/0109088].

[24] M. Beneke, G. Buchalla, C. Greub, A. Lenz and U. Nierste, Phys. Lett. B **459** (1999) 631 [arXiv:hep-ph/9808385].

[25] M. Beneke, G. Buchalla, A. Lenz and U. Nierste, Phys. Lett. B **576** (2003) 173 [arXiv:hep-ph/0307344].

[26] M. Ciuchini, E. Franco, V. Lubicz, F. Mescia and C. Tarantino, JHEP **0308** (2003) 031 [arXiv:hep-ph/0308029].

[27] A. Lenz and U. Nierste, JHEP **0706** (2007) 072 [arXiv:hep-ph/0612167].

[28] T. Inami and C. S. Lim, Progr. Theor. Phys. 65 (1981) 297 [Erratum: 65 (1981) 1772].

[29] S. Aoki *et al.* [JLQCD Collaboration], Phys. Rev. Lett. **91** (2003) 212001 [arXiv:hep-ph/0307039]. E. Dalgic *et al.*, arXiv:hep-lat/0610104; J. Shigemitsu for HPQCD Collaboration, talk at LATTICE 2006,
http://www.physics.utah.edu/lat06/abstracts/sessions/weak/s1//Shigemitsu_Junko.pdf.

[30] A. I. Vaĭnsteĭn, V. I. Zakharov, V. A. Novikov and M. A. Shifman, Sov. J. Nucl. Phys. 23 (1976) 540. M. I. Vysotskiĭ, Sov. J. Nucl. Phys. 31 (1980) 797. F. J. Gilman and M. B. Wise, Phys. Rev. D27 (1983) 1128. J. M. Flynn, Mod. Phys. Lett. A5 (1990) 877. A. Datta, J. Fröhlich and E. A. Paschos, Z. Phys. C46 (1990) 63.

[31] S. Herrlich and U. Nierste, Nucl. Phys. B **419** (1994) 292.

[32] S. Herrlich and U. Nierste, Phys. Rev. D **52** (1995) 6505; Nucl. Phys. B **476** (1996) 27.

[33] D. J. Antonio *et al.* [RBC Collaboration and UKQCD Collaboration], Phys. Rev. Lett. **100** (2008) 032001 [arXiv:hep-ph/0702042].

[34] K. Anikeev *et al.*, *B physics at the Tevatron: Run II and beyond*, [hep-ph/0201071].

[35] A. J. Buras and D. Guadagnoli, Phys. Rev. D **78** (2008) 033005 [arXiv:0805.3887 [hep-ph]].

[36] Robert E. Marshak, Riazuddin and Ciaran P. Ryan, *Theory of weak interactions in particle physics*, Wiley-Interscience, New York, 1969.

[37] A. S. Dighe, I. Dunietz, H. J. Lipkin and J. L. Rosner, Phys. Lett. B **369** (1996) 144 [arXiv:hep-ph/9511363]. A. S. Dighe, I. Dunietz and R. Fleischer, Eur. Phys. J. C **6** (1999) 647 [arXiv:hep-ph/9804253].

[38] I. Dunietz, R. Fleischer and U. Nierste, Phys. Rev. D **63** (2001) 114015 [arXiv:hep-ph/0012219].

[39] Y. Grossman and M. P. Worah, Phys. Lett. B **395** (1997) 241 [arXiv:hep-ph/9612269].

[40] G. Buchalla and A. J. Buras, Nucl. Phys. B **400** (1993) 225. M. Misiak and J. Urban, Phys. Lett. B **451** (1999) 161 [arXiv:hep-ph/9901278].

[41] Y. Grossman and Y. Nir, Phys. Lett. B **398** (1997) 163 [arXiv:hep-ph/9701313].

[42] U. Nierste, Int. J. Mod. Phys. A **21** (2006) 1724 [arXiv:hep-ph/0511125].

[43] M. Gronau and D. London., Phys. Lett. B **253**, 483 (1991). M. Gronau and D. Wyler, Phys. Lett. B **265**, 172 (1991).

[44] M. Gronau and D. London, Phys. Rev. Lett. **65**, 3381 (1990).

[45] A. Höcker, H. Lacker, S. Laplace and F. Le Diberder, Eur. Phys. J. C **21**, 225 (2001) [arXiv:hep-ph/0104062]. J. Charles *et al.* [CKMfitter Group], Eur. Phys. J. C **41**, 1 (2005) [arXiv:hep-ph/0406184]. `http://ckmfitter.in2p3.fr`

[46] M. Ciuchini *et al.*, JHEP **0107**, 013 (2001)[arXiv:hep-ph/0012308]. M. Bona *et al.* [UTfit Collaboration], arXiv:hep-ph/0509219. `http://utfit.roma1.infn.it`

[47] Y. Nir, arXiv:hep-ph/0510413.

[48] A. J. Buras, arXiv:hep-ph/9806471.

[49] G. Buchalla, A. J. Buras and M. E. Lautenbacher, Rev. Mod. Phys. **68** (1996) 1125 [arXiv:hep-ph/9512380].

[50] R. Fleischer, arXiv:hep-ph/0405091.

[51] G. Burdman and I. Shipsey, Ann. Rev. Nucl. Part. Sci. **53** (2003) 431 [arXiv:hep-ph/0310076]. I. I. Bigi, Nucl. Phys. Proc. Suppl. **185** (2008) 121 [arXiv:0808.1773 [hep-ph]].

[52] G. Buchalla, arXiv:hep-ph/0103166.

[53] A. Ali, arXiv:hep-ph/0312303.

[54] I.I. Bigi and A.I. Sanda, *CP violation*, Cambridge University Press, Cambridge, 2000. G.C. Branco, L. Lavoura and J.P. Silva *CP Violation*, Clarendon Press, Oxford, 1999. Oxford Science Publications.